The complete mitochondrial genome of the grooved carpet shell, *Ruditapes decussatus* (Bivalvia, Veneridae)

Fabrizio Ghiselli Corresp., [1] , **Liliana Milani** [1] , **Mariangela Iannello** [1] , **Emanuele Procopio** [1] , **Peter L Chang** [2] , **Sergey V Nuzhdin** [2] , **Marco Passamonti** [1]

[1] Department of Biological, Geological and Environmental Sciences, University of Bologna, Italy, Bologna, BO, Italy

[2] Department of Biological Sciences, Program in Molecular and Computational Biology, University of Southern California, Los Angeles, CA, United States

Corresponding Author: Fabrizio Ghiselli
Email address: fabrizio.ghiselli@unibo.it

Despite the large number of animal complete mitochondrial genomes currently available in public databases, knowledge about mitochondrial genomics in invertebrates is uneven. This paper reports, for the first time, the complete mitochondrial genome of the grooved carpet shell, *Ruditapes decussatus*, also known as the European clam. *R. decussatus* is morphologically and ecologically similar to the Manila clam *Ruditapes philippinarum*, which has been recently introduced for aquaculture in the very same habitats of *R. decussatus*, and that is replacing the native species. Currently the production of the European clam is almost insignificant, nonetheless it is considered a high value product, and therefore it is an economically important species, especially in Portugal, Spain and Italy. In this work we: *i)* assembled *R. decussatus* mitochondrial genome from RNA-Seq data, and validated it by Sanger sequencing, *ii)* analyzed and characterized the *R. decussatus* mitochondrial genome, comparing its features with those of other venerid bivalves; *iii)* assessed mitochondrial sequence polymorphism (SP) and copy number variation (CNV) of tandem repeats across 26 samples. Despite using high-throughput approaches we did not find evidence for the presence of two sex-linked mitochondrial genomes, typical of the Doubly Uniparental Inheritance of mitochondria, a phenomenon known in ~100 bivalve species. According to our analyses, *R. decussatus* is more genetically similar to species of the Genus Paphia than to the congeneric *R. philippinarum*, a finding that bolsters the already-proposed need of a taxonomic revision. We also found a quite low genetic variability across the examined samples, with few SPs and little variability of the sequences flanking the control region (Largest Unassigned Regions, LURs). Strikingly, although we found low nucleotide variability along the entire mitochondrial genome, we observed high levels of length polymorphism in the LUR due to CNV of tandem repeats, and even a LUR length heteroplasmy in two samples. It is not clear if the lack of genetic variability in the mitochondrial genome of *R. decussatus* is a cause or an effect of the ongoing replacement

of *R. decussatus* with the invasive *R. philippinarum*, and more analyses, especially on nuclear sequences, are required to assess this point.

AUTHOR COVER PAGE

The Complete Mitochondrial Genome of the Grooved Carpet Shell, *Ruditapes decussatus* (Bivalvia, Veneridae).

Fabrizio Ghiselli[1,*,º], Liliana Milani[1,º], Mariangela Iannello[1], Emanuele Procopio[1], Peter L. Chang[2], Sergey V. Nuzhdin[2], and Marco Passamonti[1]

[1] Department of Biological, Geological and Environmental Sciences - University of Bologna, Italy.

[2] Program in Molecular and Computational Biology, Department of Biological Sciences, University of Southern California, Los Angeles, CA, USA.

º Equal contribution

*Corresponding Author: Fabrizio Ghiselli fabrizio.ghiselli@unibo.it

Abstract

Despite the large number of animal complete mitochondrial genomes currently available in public databases, knowledge about mitochondrial genomics in invertebrates is uneven. This paper reports, for the first time, the complete mitochondrial genome of the grooved carpet shell, *Ruditapes decussatus*, also known as the European clam. *R. decussatus* is morphologically and ecologically similar to the Manila clam *Ruditapes philippinarum*, which has been recently introduced for aquaculture in the very same habitats of *R. decussatus*, and that is replacing the native species. Currently the production of the European clam is almost insignificant, nonetheless it is considered a high value product, and therefore it is an economically important species, especially in Portugal, Spain and Italy.

In this work we: *i)* assembled *R. decussatus* mitochondrial genome from RNA-Seq data, and validated it by Sanger sequencing, *ii)* analyzed and characterized the *R. decussatus* mitochondrial genome, comparing its features with those of other venerid bivalves; *iii)* assessed mitochondrial sequence polymorphism (SP) and copy number variation (CNV) of tandem repeats across 26 samples.

Despite using high-throughput approaches we did not find evidence for the presence of two sex-linked mitochondrial genomes, typical of the Doubly Uniparental Inheritance of mitochondria, a phenomenon known in ~100 bivalve species. According to our analyses, *R. decussatus* is more genetically similar to species of the Genus Paphia than to the congeneric *R. philippinarum*, a finding that bolsters the already-proposed need of a taxonomic revision. We also found a quite low genetic variability across the examined samples, with few SPs and little variability of the sequences flanking the control region (Largest Unassigned Regions, LURs). Strikingly, although we found low nucleotide variability along the entire mitochondrial genome, we observed high

47 levels of length polymorphism in the LUR due to CNV of tandem repeats, and even a LUR
48 length heteroplasmy in two samples. It is not clear if the lack of genetic variability in the
49 mitochondrial genome of *R. decussatus* is a cause or an effect of the ongoing replacement of *R.*
50 *decussatus* with the invasive *R. philippinarum*, and more analyses, especially on nuclear
51 sequences, are required to assess this point.
52
53
54
55 **Keywords: (3-10)**
56 complete mitochondrial genome; mitochondrial length polymorphism; mitochondrial repeats;
57 codon usage; bivalve molluscs; European clam; comparative mitochondrial genomics; Doubly
58 Uniparental Inheritance; mtDNA *de novo* assembly; RNA-Seq.
59

Introduction

Despite a large number of animal complete mitochondrial genomes (mtDNAs) being available in public databases (>55,000 in GenBank), up to now sequencing has been focused mostly on vertebrates (~50,000 in GenBank), and the current knowledge about mitochondrial genomics in invertebrates—with the notable exception of few model organisms (e.g. Drosophila and *Caenorhabditis elegans*)—is uneven. To better understand invertebrate mitochondrial biology—and, most importantly, mitochondrial biology and evolution in general—it is necessary to adopt a more widespread approach in gathering and analyzing data. Failing to do so would bias our knowledge toward a few taxonomic groups, with the risk of losing a big part of the molecular and functional diversity of mitochondria. Actually, despite maintaining its core features in terms of genetic content, mtDNA in Metazoa shows a wide range of variation in some other traits such as, for example, genome architecture, abundance of unassigned regions (URs)—namely regions with no assigned product (protein, RNA)—repeat content, gene duplications, introns, UTRs, and even additional coding genes (see Breton et al., 2014 for a review) or genetic elements (e.g, small RNAs, see Pozzi et al., 2017) . All this emerging diversity is in sharp contrast with the—at this point outdated—textbook notion about mtDNAs role being limited to the production of a few subunits of the protein complexes involved in oxidative phosphorylation (OXPHOS).

This paper reports, for the first time, the complete mitochondrial genome of the grooved carpet shell, *Ruditapes decussatus* (Linnaeus, 1758). *R. decussatus*—also known as the European clam—is distributed all over the Mediterranean coasts, as well as on the Atlantic shores, from Lofoten Islands (Norway) to Mauritania, including the British Isles. *R. decussatus* lives in warm coastal waters, especially in lagoons, and it is morphologically and ecologically similar to the

Manila clam *Ruditapes philippinarum*, which has been recently introduced for aquaculture in the very same habitats of *R. decussatus. R. philippinarum*, native from the Philippines, Korea, and Japan, was accidentally introduced into North America in the 1930s, and from there it was purposely introduced in France (1972), UK (1980), and Ireland (1982) for aquaculture purposes (Gosling, 2003). According to historical records, *R. decussatus* was one of the most important species for aquaculture in Europe, but overfishing, irregular yields, recruitment failure, and outbreaks of bacterial infection pushed the producers to introduce *R. philippinarum*; Italy imported large quantities of *R. philippinarum* seed from UK in 1983 and 1984. Compared to the European clam, the Manila clam turned out to be faster growing, more resistant to disease, to have a more extended breeding period and a greater number of spawning events, and to begin sexual maturation earlier (i.e. at a smaller size). Upon introduction of the more robust *R. philippinarum*, *R. decussatus* suffered a population decline in the Southwestern Europe (Arias-Pérez et al., 2015), and currently the production of the European clam is almost insignificant. Nonetheless the grooved carpet shell is considered a high value product, and therefore it is an economically important species, especially in Portugal, Spain and Italy (Gosling, 2003; Leite et al., 2013; de Sousa et al., 2014).

Molluscs in general, and bivalves in particular, exhibit an extraordinary degree of mtDNA variability and unusual features, such as: large mitochondrial genomes (up to ~47Kb), high proportion of URs (i.e. number of base pairs annotated as URs over the total mtDNA length), novel protein coding genes with unknown function, frequent and extensive gene rearrangement, and differences in strand usage (Gissi, Iannelli & Pesole, 2008; Breton et al., 2011; Ghiselli et al., 2013; Milani et al., 2014b; Plazzi, Puccio & Passamonti, 2016). Moreover, mitochondrial genome size varies among bivalves because of gene duplications and losses (Serb & Lydeard,

2003; Passamonti et al., 2011; Ghiselli et al., 2013), and sometimes genes are fragmented as in the case of ribosomal genes in oysters (Milbury et al., 2010). The most notable feature of bivalve mtDNA is the Doubly Uniparental Inheritance (DUI) system of transmission (Skibinski, Gallagher & Beynon, 1994a,b; Zouros et al., 1994a,b). Under DUI, two different mitochondrial lineages (and their respective genomes) are transmitted to the progeny: one is inherited from the egg (female-transmitted or F-type mtDNA), the other is inherited from the spermatozoon (male-transmitted or M-type mtDNA). Following fertilization, the early embryo is heteroplasmic, but the type of mitochondria present in the adult is tightly linked to its sex. Females are commonly homoplasmic for F, while males are heteroplasmic with the following distribution of mtDNA types: the germ line is homoplasmic for the M-type (which will be transmitted via sperm to male progeny), the soma is heteroplasmic to various degrees, depending on tissue type and/or species (Ghiselli, Milani & Passamonti, 2011; Zouros, 2013). To date, the only known animals exhibiting DUI are about 100 species of bivalve molluscs (Gusman et al., 2016). This natural and evolutionarily stable heteroplasmic system can be extremely useful to investigate several aspects of mitochondrial biology (see Passamonti & Ghiselli, 2009; Breton et al., 2014; Milani & Ghiselli, 2015; Milani, Ghiselli & Passamonti, 2016). Indeed, despite the fact that many aspects of DUI are still unknown, there is evidence that DUI evolved from a strictly maternal inheritance (SMI) system (Milani & Ghiselli, 2015; Milani, Ghiselli & Passamonti, 2016), by modifications of the molecular machinery involved in mitochondrial inheritance, through as-yet-unknown specific factors (see Diz, Dudley & Skibinski, 2012; and Zouros, 2013 for proposed models). The detection of DUI is not a straightforward process, especially using PCR-based approaches: given that the divergence between F and M genomes is often comparable to the distance between mtDNAs of different classes of Vertebrates, primers may fail to amplify one of the two mtDNAs,

yielding a false-negative result. Moreover, M-type mtDNA can be rare in somatic tissues, so it may be difficult to amplify from animals sampled outside of the reproductive season, when gonads are absent (thoroughly discussed in Theologidis et al., 2008). High-throughput sequencing (HTS) approaches can overcome such problems, because a prior knowledge of the mtDNA sequence is not needed, and low-copy variants can be easily unveiled (see for example: Ju et al. 2011; King et al. 2014). Until now, HTS has been scarcely utilized to study mitochondrial transcriptomes and genomes (Pesole et al., 2012; Smith, 2013), even if it showed very good potential (Lubośny et al., 2017/2; see for example Yuan et al., 2016). In this work we: *i)* assembled *R. decussatus* mitochondrial genome from RNA-Seq data, and validated it by Sanger sequencing, *ii)* analyzed and characterized *R. decussatus* mitochondrial genome, comparing its features with those of other venerid bivalves; *iii)* assessed mitochondrial sequence polymorphism (SP) and structural variants—copy number variation (CNV) of tandem repeats—among the sampled animals.

Materials & Methods

Sampling

The 26 *Ruditapes decussatus* specimens used in this study were collected from the Northern Adriatic Sea, in the river Po delta region (Sacca di Goro, approximate GPS coordinates: 44°50’06”N, 12°17’55”E) at the end of July 2011, during the spawning season. Each individual was dissected, and gonadal liquid collected with a glass capillary tube. All the samples showed ripe gonads, consistently with the time of the year when the sampling occurred. The gonadal liquid was checked under a light microscope to assess the sex of the individual, and to make sure

that the sample consisted of mature gametes. Both the gamete samples and the clam bodies were flash-frozen in liquid nitrogen, and stored at -80ºC, until nucleic acid extraction. Supplementary Table 1 shows the sample list, and details about data availability.

RNA-Seq

In total, 12 samples (6 males and 6 females) were used for RNA-Seq. Total RNA extraction and library preparation were performed following the protocol described in Mortazavi et al. (2008), with the modifications specified in Ghiselli et al. (2012). The 12 samples were indexed, pooled and sequenced in two lanes (two technical replicates) of Illumina GA IIx, using 76bp paired-end reads.

De Novo Assembly

The mitochondrial genome of *R. decussatus* was not available in the databases, so we used the transcriptome data to generate a draft to be used as a guide for Sanger sequencing. Illumina reads from all 12 samples were pooled and compared to a set of 20 bivalvia mitochondrial genomes to identify reads with mitochondrial origin. Alignment was done using BLASTN. All reads with similarity yielding E-value < 1E-5 were then assembled into contigs using the A5 pipeline (version 2013032; Tritt et al, 2012) and joined into scaffolds using CAP3 (Huang & Madan, 1999). For the quality check step, we applied a PHRED Q-score cutoff threshold of 33; the other A5 parameters were set as default. CAP3 was run with default settings as well.

174 *Sanger Validation*

175 In total, 14 *R. decussatus* samples from the same collection campaign—sexed, and stored at -
176 80°C—were used for DNA extraction. DNA from the gonadic tissue was extracted using the
177 Qiagen DNeasy kit. Primers for mtDNA amplification were designed based on contigs obtained
178 from RNA-Seq matching venerid mtDNA sequences, then the "primer walking" method was
179 used to Sanger-sequence the complete mitochondrial genome of *R. decussatus*. The primers were
180 designed with the software Primer3 (Rozen & Skaletsky, 2000) and tested on several samples,
181 then a female was chosen as reference sample for Sanger validation of mtDNA *de novo*
182 assembly. In addition, we amplified the Largest Unassigned Region (LUR) of 13 females to
183 assess its variability (see Results and Discussion). The list of the primers and their sequences are
184 reported in Supplementary Table 2. PCR reactions were performed in a final volume of 50µl
185 using the GoTaq Flexi DNA Polymerase Kit (Promega), on a 2720 Thermal Cycler (Applied
186 Biosystem). The PCR reactions were set as follows: initial denaturation 95°C for 1 min, then 30
187 cycles of amplification (denaturation 95°C for 1 min, annealing 48- 60°C for 1 min, extension
188 72°C for 1 min/kb), then the final extension at 72°C for 5 min. PCR products were checked by
189 electrophoretic run on 1% agarose gel, and then purified using the DNA Clean & Concentrator-
190 25 kit (Zymo Research).

191 Sanger sequencing was performed by Macrogen Inc. (http://www.macrogen.com).
192 Sequences were aligned with the software MEGA 6.0 (Tamura et al., 2013), using the contigs
193 obtained by RNA-seq as a reference.

194

Annotation

Open Reading Frames (ORFs) were identified with ORF finder (Wheeler et al., 2005). Alternative start codons were considered functional because they are common in Bivalvia. ORFs were annotated starting from the first available start codon (ATG, ATA or ATC) downstream of the preceding gene, and ending with the first stop codon in frame (TAA or TAG). tRNA genes and their structure were identified with MITOS (Bernt et al., 2013) and ARWEN (Laslett & Canback, 2008). Secondary structures were predicted using the RNAFold Server, included in the ViennaRNA Web Services (http://rna.tbi.univie.ac.at/; Gruber et al., 2008); the folding temperature was set at 16°C which is the average annual temperature of the water from which the *R. decussatus* specimens used in this work were fished (download RNAFold results from figshare: https://ndownloader.figshare.com/files/8387672). tRNAs and other secondary structures were drawn with the software Varna GUI (Darty, Denise & Ponty, 2009). Ribosomal small subunit (*rrnS*) and large subunit (*rrnL*) were identified with BLASTN, and annotated considering the start and the end of the adjacent genes as the boundaries of the rRNA genes. Non-genic regions were annotated as Unassigned Regions (URs). In order to identify the putative D-loop/control region (CR), we analyzed the LUR with the MEME suite (Bailey et al., 2009) to find DNA motifs using the following bivalve species as comparison: *Acanthocardia tuberculata*, *Arctica islandica*, *Coelomactra antiquata*, *Fulvia mutica*, *Hiatella arctica*, *Loripes lacteus, Lucinella divaricata, Lutraria rhynchaena, Meretrix lamarckii* (F-type), *Meretrix lamarckii* (M-type), *Meretrix lusoria, Meretrix lyrata, Meretrix meretrix, Meretrix petechialis, Moerella iridescens, Nuttallia olivacea, Paphia amabilis, Paphia euglypta, Paphia textile, Paphia undulata, Ruditapes philippinarum* (F-type), *Ruditapes philippinarum* (M-type*), Semele scabra, Sinonovacula constricta, Solecurtus divaricatus, Solen grandis, Solen strictus, Soletellina diphos*

and the sea urchin *Strongylocentrotus purpuratus* (Echinoidea, Strongylocentrotidae). The list of the species used in the phylogenetic analysis and in the comparative analyses of DNA motifs, sequence similarity, and gene order are available in Supplementary Table 3. The GOMo (Gene Ontology for Motifs; Buske et al., 2010) tool of the MEME suite was used to assign GO terms to the motifs discovered.

The number of repeats in the LUR of the reference sample (F4) was calculated with tandem repeat finder (http://tandem.bu.edu/trf/trf.html), since the complete LUR sequence was available (download tandem repeat finder results from figshare: https://ndownloader.figshare.com/files/8387666). In the other cases, in which the LUR could not be sequenced without gaps, the number of repeats was inferred from agarose gel electrophoresis.

Other Analyses

Comparisons among venerid complete mtDNAs were performed with BLAST Ring Image Generator (BRIG, Alikhan et al., 2011) and Easyfig (Sullivan, Petty & Beatson, 2011). Descriptive statistics were obtained with MEGA v6.0 (Tamura et al., 2013), except for the codon usage table, which was obtained with the Sequence Manipulation Suite (Stothard, 2000). Sequence polymorphism (SP) assessment from RNA-Seq reads was performed with the Genome Analysis Toolkit (GATK, McKenna et al., 2010), with the Sanger-sequenced mtDNA as reference. For SP discovery and genotyping we used standard hard filtering parameters or variant quality score recalibration (DePristo et al., 2011). The MitoPhast pipeline (Tan et al., 2015) was used to obtain the Maximum Likelihood (ML) tree, which was visualized with Evolview v2 (He et al., 2016). Briefly, MitoPhast takes as input GenBank files (.gb), extracts the coding sequences, profiles the sequences with Pfam (Finn et al., 2016) and PRINTS (Attwood et al.,

2003), performs a multiple sequence alignment with Clustal Omega (Sievers et al., 2011), removes poorly aligned regions with trimAl (Capella-Gutiérrez, Silla-Martínez & Gabaldón, 2009), concatenates the coding sequences, performs data partitioning and model selection, and then carries out a ML analysis using RAxML (Stamatakis, 2014). The species used in the ML analysis, and their GenBank Accession Numbers are listed in Supplementary Table 3. Amino acid sequences of three different *cox3* ORFs inferred from Sanger sequencing and GATK polymorphism data were analyzed with InterProScan (Jones et al. 2014).

Results

De Novo Assembly and Sanger Validation

Despite using HTS on extracts of ripe gonads (i.e. mature gametes), and multiple assembly strategies (see Discussion for details) we could not find evidence for DUI. The *de novo* assembly process produced 9 contigs, of which 8 included multiple genes, and one included a single gene (see Table 1). The sequences of the contigs in FASTA format are available on figshare (https://ndownloader.figshare.com/files/8906839). In four cases (Contigs 1, 3, 6, and 7) a clear polyadenylation signal was present, in other four cases (Contigs 2, 5, 8, and 9) it was not. Contig 4, the only one including a single gene (*cox3*), ends with just 8 As, so it is not clear if a polyadenylation signal is present in this case. In Contig 7 (that includes *cox2, tRNA-Ile, nd4L, nd2, nd1, tRNA-Leu1*, and *cox1* genes) there is a polyadenylation signal (56 As) after the *cox2* gene.

The 9 contigs were used as a scaffold for the primer walking procedure used for Sanger validation of the *de novo* assembly. We first tried to connect the contigs designing primers close to the 5' and 3' ends of each contig and pairing them following the gene order of Paphia, because

the sequence of genes in the contigs suggested that *R. decussatus* gene order might have been similar. During such process, Contig 1 turned out to be a chimeric assembly between two non-contiguous portions of the mtDNA, one including *atp6, nd3,* and *nd5*, the other including *cox1, tRNA-Leu1, nd1, nd2,* and *nd4L*. Once we amplified and sequenced the portions of mtDNA between the contigs, we proceeded with the Sanger resequencing of the remaining parts.

Annotation and mtDNA Features

The mitochondrial genome contains 13 protein-coding genes, and in the reference female is 18,995 bp long (Figure 1); the gene arrangement and other details are shown in Table 2. All genes are located on the heavy strand, and in addition to the classic start codon ATG (Met), the alternative start codons ATA (Met) and ATC (Ile) are present. The most frequently used start codons are: ATA (*cox1, nd1, nd4L, cox2, cob, atp8, nd4*), and ATG (*nd2, atp6, nd3, nd5, nd6, cox3*). The stop codons found are TAG (*cox1, nd2, nd4L, cox2, cytb, nd4*) and TAA (*nd1, atp6, nd3, atp8, nd6*). The *nd4* gene has an incomplete stop codon (TA-). 22 tRNA genes were identified, including two tRNAs for leucine, tRNA-Leu1(TAG) and tRNA-Leu2(TAA), and two for serine, tRNA-Ser1(TCT) and tRNA-Ser2(TGA), both showing degenerate D-arm branches. tRNA structures are shown in Supplementary Figure 1. The two rRNAs, *rrnS* and *rrnL*, were both identified: the *rrnS* is located between *cox3* and *cox1*, while *rrnL* is between *cytb* and *atp6*. Unassigned Regions (URs) were identified on the basis of unannotated spaces between different genes; we found 24 URs (Table 3).

The analysis of the nucleotide composition points out that the mitochondrial genome of this bivalve species exhibits high A+T content, totaling 63% versus 37% G+C. The minimum values of A+T are found in *cytb* (60.1%) and *nd4* (61%). The nucleotide composition of every gene is

shown in Table 4. According to the analysis above, both A and T occur very frequently at the third position of codons (64.6% on average of A+T), while the less frequent base in third position is C (12%). The most used codons are UUU (Phe), counted 269 times, and UUA (Leu) counted 210 times (6.78% and 5.29% of the total, respectively), while the less used codons are CGC (Arg) counted 6 times (0.15%), ACC (Thr) and CCG (Pro) each counted 16 times (0.4%) (Table 5). Only in 4 cases over 20 (Lys, Leu, Gln, Val), the most frequently used codon matches the correspondent mitochondrial tRNA anticodon.

The UR11 is the Largest Unassigned Region (LUR) and is located between *atp8* and *nd5* (Figures 1 and 2A). The LUR of the female used for whole mtDNA Sanger sequencing (i.e. the reference female, F4) is 2,110 bp long, and includes 6.5 repeated sequences—each repeat having a length of 54 bp—localized in the 3' region of the LUR, just upstream the *atp8* gene (Figure 2A). DNA secondary structure analysis predicted 3 stem-loop structures in such region (Figure 2B and supplementary files on figshare: https://ndownloader.figshare.com/files/8387672), with a change in Gibbs free energy (ΔG) of -71.38 Kcal/mol. We also amplified and sequenced the LUR of 13 more females. We were not able to completely sequence LURs longer than 2,110 bp, because of the known difficulties in Sanger sequencing of regions including multiple repeats. The sequence alignment of the 13 LURs is available for download from figshare (https://ndownloader.figshare.com/files/8360789). LUR lengths, inferred from gel electrophoresis, are reported in Table 6, and they range from 2,000 to 5,000 bp. Two females (F3 and F17) showed length heteroplasmy of the LUR. The portion of the genome occupied by URs varies between 14.11% and 29.38%, depending on LUR length. The analysis with MEME (output shown in Supplementary Figures 2 and 3) unveiled two motifs (Figure 2C) that show a strong conservation within the Veneridae family, and with *S. purpuratus*. The sea urchin was

310 included in the analysis because Cao et al. (2004) reported a match between some motifs found
311 in the CR of the marine mussels *Mytilus edulis* and *Mytilus galloprovincialis* with regulatory
312 elements of the sea urchin CR. Accordingly, the search with GOMo assigned a series of GO
313 terms related to transcription to the two motifs (Supplementary Table 4).
314
315 *Polymorphism*
316 Table 7 (top) shows the statistics associated with the SP analysis performed with GATK on the
317 12 samples used for RNA-Seq, with the Sanger-sequenced mtDNA as reference. Overall, 257
318 SPs were called, of which 145 (56.4%) were located in coding sequences (CDS). Interestingly,
319 most of the SPs were called because of private alleles of one single male specimen (mRDI01).
320 More in detail, 151 SPs out of 257 (58.7%) along the whole mtDNA sequence, and 103 SPs out
321 of 145 (71%) in CDS, were private of mRDI01. In CDS, if we exclude the SPs associated with
322 this male, the number of polymorphisms drops to 42 over 14,920 bp of coding mtDNA (GATK
323 output in VCF format and a detailed list of SPs in tabular format is available on figshare:
324 https://ndownloader.figshare.com/files/8902537), of which 18 are represented by indels, 6 of
325 which are located in 4 different coding genes: one each in *cox1*, *cytb*, and *nd5*, plus 3 in *cox3*
326 (see Table 8). A file showing the ORF generated by the different variants of *cox3*, and
327 alignments between them is available on figshare
328 (https://ndownloader.figshare.com/files/8402471). Table 7 (bottom) shows the number of SPs in
329 males, in males except mRDI01, and in females both along the whole mtDNA, and in CDS. The
330 number in brackets represent the number of private SPs for each category.
331
332 *Comparison with Other Veneridae*

Figure 3 shows the *R. decussatus* mtDNA map (external gray circle), and the BLASTN identity (colored inner circles) with complete mtDNAs of other 10 venerid species (see list in Supplementary Table 3). Figure 4 shows the ML tree obtained with the MitoPhast pipeline; the complete input and output of this analysis is available on figshare (https://ndownloader.figshare.com/files/8360792). Figure 5 shows the variation in gene order between *R. decussatus* and *P. euglypta* (Figure 5A), *M. lamarckii* F-type (Figure 5B), *R. philippinarum* F-type (Figure 5C), and among all the 4 species (Figure 5D).

Discussion

RNA-Seq-guided Sequencing of mtDNA

The *de novo* assembly of the mtDNA from RNA-Seq data turned out to be informative, simplifying the primer walking procedure used for Sanger sequencing. Only one conting (Contig 1) resulted to be a chimeric sequence obtained by the misassembly of two smaller contigs. Most of the contigs (8 out of 9) contained more than one gene, and most of the tRNA genes were included in the *de novo* assembly. Except for *tRNA-Pro, tRNA-Ile,* and *tRNA-Leu1*, all the other tRNA genes are organized in two big clusters: a 13-gene cluster positioned between *cox3* and *nd6*, and a 6-gene cluster between *nd6* and *nd4*. The assembly retrieved 6 out of 13 tRNAs from the first cluster (missing *tRNA-Gly, tRNA-Glu, tRNA-Asn, tRNA-Thr, tRNA-Cys, tRNA-Ala,* and *tRNA-Ser1*), and 4 out of 6 tRNAs from the second cluster (missing *tRNA-Met* and *tRNA-Asp*). All the tRNA genes not located in these two clusters (*tRNA-Pro, tRNA-Ile,* and *tRNA-Leu1*) were included in the contigs. The presence of a clear polyadenylation signal in 4 of the assembled contigs (see Table 1) seems to indicate the existence of multiple polycistronic transcripts. It is also noteworthy that poly-A sequences seem to be absent in contigs having tRNA of rRNA genes

356 at one end (Contigs 2, 5, 8 and 9). This could be either an evidence supporting the "tRNA
357 punctation model" of RNA processing proposed by Ojala et al. (1981) for human mitochondria,
358 or a result of difficulties in sequencing/assembly of such regions. More analyses are required to
359 address this point.
360
361 *General Features*
362 The size of the fully Sanger-sequenced mitochondrial genome of *R. decussatus* (reference female
363 F4) is of 18,995 bp, and it includes 13 protein-coding genes, 22 tRNAs and 2 rRNAs. Our data
364 support the presence of the *atp8* gene in the mtDNA of *R. decussatus; atp8* has been reported as
365 missing in several bivalve species, however more accurate searches often led to the identification
366 of the gene, so, in most cases, the alleged lack of *atp8* is likely ascribable to annotation
367 inaccuracies due to the extreme variability and the small size of the gene (Breton, Stewart &
368 Hoeh, 2010; Breton et al., 2014; Plazzi, Puccio & Passamonti 2016).
369 The mitochondrial genome of *R. decussatus* shows a high content of A-T (63%), a common
370 feature in bivalve mtDNAs; moreover, T is the most common nucleotide at the third codon base
371 (64.6%). The most common codon is UUU (Phe), which is also the most commonly used in
372 bivalves, as well as in other invertebrates (Passamonti et al., 2011).
373
374 *Codon Usage*
375 As shown in Table 5, in 16 cases out of 20, the most frequently used codon does not correspond
376 to the anticodon of the inferred tRNA. In other words, there is not a correspondence between the
377 most abundant codons and the anticodons of the 22 mitochondrial tRNAs. According to the
378 "wobble hypothesis"—first proposed by Francis Crick (1966)— the conformation of the tRNA

anticodon loop enables some flexibility at the first base of the anticodon, so a Watson-Crick type of base pairing in the third position of the codon is not strictly necessary. This allows an amino acid to be correctly incorporated by ribosomes even if the tRNA is not fully complementary to the codon; according to Crick, this explains the degeneracy of the genetic code. This feature is particularly interesting in the light of the debate about natural selection acting at synonymous sites: since the early 1980s, evidence of a correlation between synonymous codon usage and tRNA abundances started accumulating. According to these authors, synonymous codon usage is biased to match skews in tRNA abundance, as a result of selective pressure maximizing protein synthesis rates (reviewed in Chamary, Parmley & Hurst, 2006). Following this rationale, the results here reported and data from other marine bivalves and metazoans (Yu & Li, 2011; Passamonti et al., 2011) would suggest that in some mitochondrial genomes translation efficiency is not maximized, and this observation deserves further investigation.

Length and Sequence Polymorphism

The mtDNA of *R. decussatus* has a high proportion of URs mostly depending on the length of the LUR (Table 6); on average, bivalve mtDNAs have 1.7x the amount of URs in respect to other analyzed Metazoa (Ghiselli et al., 2013), and it is still unclear whether there is an accumulation of non-functional sequences in bivalve mtDNA due to genetic drift, or if such URs are maintained by natural selection because they contain—so far unknown—functional elements (see for example Milani et al., 2013, 2014b; Breton et al., 2014; Pozzi et al., 2017). The LUR of *R. decussatus* most likely includes the mitochondrial CR, as indicated by the presence of two motifs (Figure 2C, Supplementary Figures 3 and 4) similar to two regulatory elements identified in the sea urchin CR. These two motifs are the same identified in previous analyses on the clam

R. philippinarum and the mussel *Musculista senhousia* (Ghiselli et al., 2013; Guerra, Ghiselli & Passamonti, 2014) so they are conserved across distant bivalve taxa, and the GO terms associated with such motifs are related to transcriptional control (Supplementary Table 4). An interesting feature of *R. decussatus* LUR is its variable length (Table 6), most likely due to different repeat content. As a matter of fact, the very same repeat sequence was present in every LUR, and our data strongly suggest that LUR length variation is actually due to repeat CNV (see supplementary files on figshare: https://ndownloader.figshare.com/files/8387666 and https://ndownloader.figshare.com/files/8360789), as observed in other bivalve species (see for example Ghiselli et al., 2013; Guerra, Ghiselli & Passamonti, 2014). Tandem repeats have been also reported in the mitochondrial genomes of the bivalves *Acanthocardia tuberculata (Dreyer & Steiner, 2006)*, *Placopecten magellanicus (La Roche et al., 1990)*, *Moerella iridescens*, *Sanguinolaria olivacea*, *Semele scaba*, *Sinonovacula constricta*, *Solecurtus divaricatus* (Yuan et al., 2012), *Ruditapes philippinarum (Ghiselli et al., 2013)*, and *Musculista senhousia* (Guerra, Ghiselli & Passamonti, 2014). These repeats are believed to arise from duplications caused by replication slippage (Buroker et al., 1990; Hayasaka, Ishida & Horai, 1991; Broughton & Dowling, 1994). The tandem repeats found at the 3' end of *R. decussatus* LUR are predicted to form a secondary structure (see Figure 2B, and supplementary files on figshare) composed by multiple stem-loops, which obviously increase in number with the increment of the number of tandem repeats. The effect, if any, of tandem repeats in mtDNA is unknown: since the repeats are almost always localized in proximity of the CR, they might interact with regulatory elements—or even contain some—influencing replication and/or transcription initiation, and such interactions might also be altered by the formation of secondary structures (Passamonti et al., 2011; Ghiselli et al., 2013; Guerra, Ghiselli & Passamonti, 2014).

We assessed the genetic variability of *R. decussatus* mtDNA using two different approaches: by SNP calling in CDS (RNA-Seq data on 12 individuals), and by analysis of the LUR (Sanger sequencing of 14 individuals). The CR and its flanking regions are known to be hypervariable, so they are commonly used to assess polymorphism at low taxonomic levels. Our data strongly support a very low genetic variability: the number of SNPs in CDS is 145, of which 103 are private of a single individual (mRDI01)—thus reducing the number to 42—while the number of variable sites in the analyzed LURs is 98 over 3,095 aligned positions. Considering the known variability of mtDNA in bivalves (Gissi, Iannelli & Pesole, 2008; Ghiselli et al., 2013; Breton et al., 2014; Plazzi, Puccio & Passamonti, 2016), this is a surprising result. Even more if we compare the results of the present work to a methodologically identical analysis performed on 12 *R. philippinarum* samples from the Pacific coast of USA, performed by Ghiselli et al. (2013): in that work, GATK yielded 194 SNPs in the M-type mtDNA and 293 in the F-type. Strikingly, the 12 *R. philippinarum* samples analyzed were actually two families (6 siblings + 6 siblings). This means that randomly sampled individuals of *R. decussatus* used in this work showed a much lower mtDNA variability than *R. philippinarum* siblings. A previous analysis on the *cox1* gene of *R. decussatus* reported a nucleotide diversity (π) of 0.15 for a population from the Northern Adriatic Sea (Cordero, Peña & Saavedra, 2014). Another analysis on the same gene of *R. philippinarum* from the same range resulted in a π=0.25 (Cordero et al., 2017), so *R. decussatus* has a lower nucleotide diversity at the *cox1* locus. The difference between the variability in mtDNA of *R. decussatus* that we are reporting here and that of *R. philippinarum* reported in Ghiselli et al. (2013) appears to be more marked. It is known that the genetic variability of *R. philippinarum* in the Adriatic Sea is lower than in populations from its native range in Asia (Cordero et al., 2017), probably because of the bottlenecks that this species had to go through

448 during the multiple colonization events. The introduction in North America from Asia happened
449 first (in the 1930s), and from there the Manila clam was introduced in Atlantic Europe (in the
450 1970s and 1980s), and lastly into the Adriatic Sea (1983 and 1984), and it is plausible that the
451 genetic diversity decreased at each introduction event. Accordingly, Cordero et al. (2017)
452 observed that *R. philippinarum* genetic variability in Europe is lower compared to that of the
453 Pacific coast of the USA, so the samples analyzed in Ghiselli et al. (2013) could have been more
454 polymorphic than those analyzed in Cordero et al. (2014), thus explaining the more pronounced
455 differences in genetic variability between the Manila clam and the European clam discussed
456 above. In any case, all the available data point to a lower genetic diversity of *R. decussatus*
457 mtDNA, and it would be interesting to know whether it is a cause or an effect of the ongoing
458 replacement of *R. decussatus* with the invasive *R. philippinarum*. It will also be important to
459 investigate genetic variability of the nuclear genes, especially after Cordero et al. (2014) reported
460 contrasting levels of differentiation between mitochondrial and nuclear markers.
461 With respect to SNP effects, we found 6 indels in CDS, 2 of which do not cause frameshift, but a
462 simple insertion/deletion of 1 amino acid (SNP_1698, and SNP_17619, see Table 8). Of the
463 remaining 4, SNP_6364 and SNP_10449 consist of a deletion and an insertion of a single T in
464 two homopolymeric sequences (CTTTTTTT and CTTTTTT, respectively), raising the possibility
465 of a sequencing error. In any case, the two SNPs yield a shorter CDS (*cytb* and *nd5*,
466 respectively), and are present at relatively low frequencies in the specimens carrying them,
467 except for SNP_6364 which has a frequency of 80% in fRDI04. The *cox3* gene shows 3 SNPs:
468 the first one, SNP_17619, does not cause a frameshift, and results in the deletion of 1 alanine
469 residue, and its frequency in mRDI01 is 97%. The second one, SNP_17621, consists of a
470 deletion of a G with respect to the reference sequence, which is the Sanger-sequenced mtDNA of

sample F4; all the individuals analyzed with RNA-Seq carry this deletion except for mRDI01 which, at that position, has the same sequence of the reference mtDNA (reference-like allele frequency in mRDI01 = 99%). The third indel, SNP_17624, consists of an insertion of two nucleotides, and its frequency in mRDI01 is 99%. So, basically, for *cox3* we have three types of sequences: *i)* the Sanger-sequenced reference, which yields a 966 bp (321 aa) ORF; *ii)* a sequence found in 11/12 of samples analyzed with RNA-Seq (except mRDI01) that carries a single-nucleotide deletion (SNP_17621), and yields a 963 bp (320 aa) ORF; *iii)* a sequence, private of mRDI01, which is obtained by combining SNP_17624 and SNP_17621 (both 99% of frequency, so most likely co-occurring), which produces a 963 bp (320 aa) ORF. Interestingly, the ORFs obtained from the sequences described in *ii)* and *iii)*, are almost identical, namely the sequence obtained by RNA-seq in 11/12 samples and the sequence obtained by RNA-Seq in mRDI01 are basically the same, and differ from the Sanger-sequenced reference, yielding an amino acid sequence that differs in the last 35 residues (all data available in supplementary files on figshare: https://doi.org/10.6084/m9.figshare.4970762.v3). Given this consistent difference between the sequence obtained by Sanger-sequencing of DNA, and those obtained by RNA-Seq, it is tempting to speculate that this difference might be caused by RNA editing, a mechanism observed in mtDNA of some animals (Lavrov & Pett, 2016), and recently reported to be common in cephalopods (Liscovitch-Brauer et al., 2017). Actually, Liscovitch-Brauer et al. (2017) reported only A-to-I editing, which is not the kind of change we are observing here, but other types of editing are known across eukaryotes (see Gott & Emeson, 2000 for a review), and some others, still unknown, might exist as well. Post-transcriptional modifications (thus including RNA-editing) are still poorly understood mechanisms, but they appear to be responsible for most of the mitochondrial gene expression regulation (Scheibye-Alsing et al.,

494 2007; Scheffler, 2008; Milani et al., 2014a). What we propose here is a pure conjecture, but we
495 think in the future it might be worthy to investigate mitochondrial transcriptomes looking for
496 such kind of "unexpected" biological features.
497 Interestingly, in contrast with a low nucleotide variability along the entire mitochondrial genome,
498 we observed a pretty high polymorphism in LUR length due to CNV of tandem repeats, and even
499 a LUR length heteroplasmy: two females yielded two electrophoretic bands each (~2,100 and
500 ~3,500 bp in F3; ~2,500 and ~3,500 bp in F17; see Table 6). A possible explanation is that the
501 diversity (CNV) detected in the LURs could be recent: the accumulation of nucleotide variation
502 at different sites along the mitochondrial genome needs time, while the kind structural variability
503 we observed can be achieved in few generations (or even one) considering that replication
504 slippage is common in repeat-rich regions.
505
506 *Phylogenetic Relationship with R. philippinarum*
507 Despite *R. decussatus* and *R. philippinarum* being morphologically similar and being ascribed to
508 the same genus, the results here reported clearly show that they are quite different both for
509 mtDNA sequence (Figures 3 and 4) and mtDNA gene arrangement (Figure 5). This is an unusual
510 finding, even among bivalves, which are known to be fast-evolving for these characters. This
511 may point to the fact that these two species are less related than previously thought. Actually,
512 this is not the first clue that *R. decussatus* and *R. philippinarum* are quite different genetically, as
513 allozyme electrophoresis (Passamonti, Mantovani & Scali, 1997, 1999) and satellite DNA
514 content (Passamonti, Mantovani & Scali, 1998) pointed out. More in-depth analyses are
515 therefore needed to correctly trace the phylogenetic relationships of these two Ruditapes species,

516 which may eventually end up in two different Genera. As shown in Figures 3, 4 and 5, the Genus
517 Paphia is the most similar to *R. decussatus*.
518
519 *Presence/absence of DUI*
520 We could not find evidence for sex-specific mtDNAs, typical of DUI. As stated in the
521 Introduction, the search for DUI is not a straightforward process. HTS can help thanks to a much
522 deeper sequencing coverage (in respect to the cloning-and-Sanger-sequencing approach), and
523 because it overcomes the problem of primer specificity, a limitation of the classical approach.
524 One possible concern about using HTS approaches based on short reads in presence of DUI is
525 about the ability of softwares to detect divergent reads and assembly them correctly. More
526 specifically, one could ask what is the divergence threshold under which the assemblers are not
527 able to partition the contigs into two sex-linked groups. We do not know such threshold, but we
528 tried different assembly strategies trying to retrieve sex-specific mtDNA sequences from our
529 data. Other than the approach reported in Materials and Methods (which is the one that produced
530 the data reported here), we tried other techniques. After identifying reads that blasted to bivalve
531 mitochondrial sequences present in GenBank and discarding all the other reads, we generated
532 A5+CAP3 assemblies: *i)* for each of the samples (obtaining 12 separate assemblies), and *ii)*
533 pooling the 6 males together and the 6 females together, and assembling the two sex-specific
534 pools. Both these approaches did not show evidence of sex-specific mtDNAs. Then we took the
535 assembly obtained from the females and removed the reads from each of the samples that
536 mapped (<8 mismatches) to these sequences. We then used the remaining reads as A5 input. The
537 program could not assemble anything. Lastly, we tried the software MetaVelvet (Namiki et al.
538 2012)—that assembles metagenomes—on all the reads matching bivalve mtDNAs, and only one

539 genome was produced. After all these alternative approaches failed to find two sex-linked
540 mtDNAs, we decided to proceed with the assembly as indicated in Materials and Methods,
541 because it was the technique that yielded the best quality contigs, most likely because using the
542 reads from all 12 the individuals granted a higher coverage of the mtDNA. Given these results,
543 we can propose three different explanations.

544 1) *R. decussatus* is characterized by strictly maternal inheritance of mitochondria, so a male-
545 transmitted mtDNA is not present in this species.
546 2) The divergence between the two sex-specific mtDNAs is too low to be detected. This
547 could be the outcome of two different situations.
548 *a.* DUI is very young in this species, so the two sex-linked mtDNAs did not have the
549 time to diverge.
550 *b.* A role-reversal event occurred recently. Role reversal (a.k.a. "route reversal" or
551 "masculinization") is a process—observed so far only in species of the Mytilus
552 complex—by which F-type genomes invades the male germ line becoming
553 sperm-transmitted, thus turning into M-type mtDNAs (Hoeh et al. 1997). This
554 event actually resets to zero the divergence between F- and M-type, although
555 substantial differences in the control regions were reported between the original
556 F-type and the "masculinized" one (see Zouros 2013 for a thorough review). The
557 hypothesis that role reversal could have occurred multiple times in the
558 evolutionary history of bivalves and could have led to the complete replacement
559 of M or F mtDNAs in several species was proposed by Hoeh et al. (1996) to
560 explain the scattered phylogenetic distribution of DUI across Bivalvia. Indeed,
561 according to the hypothesis of a single origin, DUI arose >400 Mya,

approximately at the origin of Autolamellibranchia, but, as said, such hypothesis requires the assumption of multiple role-reversal and/or DUI loss events in several branches of the bivalve tree (see Zouros, 2013 for a detailed discussion). Recently, a multiple origin of DUI was proposed (Milani et al., 2013; Milani et al., 2014b; Milani, Ghiselli & Passamonti, 2016; Mitchell et al., 2016), and in such case there would be no need of multiple role-reversal events to explain its phylogeny. In our opinion, until further evidence will be provided, role-reversal should not be considered a rule, but rather an exception. Of course, we cannot rule out that a masculinization event might have occurred in *R. decussatus*, so this hypothesis must be taken into consideration.

3) In our data, even if there is no clear evidence of a male-specific mtDNA, a male sample (mRDI01) clearly stood out from the others, both males and females (see Table 7). Overall, the divergence between mRDI01 and the other 11 samples calculated considering its private SPs is of 151 sites over 18,995 bp (considering the whole mtDNA), and of 103 sites over 14,920 bp (considering only CDS). In both cases the divergence is very low (0.8% and 0.7%, respectively), which explains why the mtDNA of mRDI01, although different, was not assembled as a separate genome. We have no sufficient data to evaluate if such divergence is normal within *R. decussatus* populations, but considered the variability usually observed in bivalves, we find the difference unsurprising. On the contrary, the lack of variability among the other 11 samples is remarkable. For these reasons, we are inclined to believe that mRDI01 divergence is compatible with hypotheses 1) and 2). That said, there still could be a third, quite

584 conjectural, hypothesis by which these data might indicate an incipient DUI, not yet fixed
585 in the population.
586 All in all, we have a preference for the first explanation, but the present data are not sufficient to
587 exclude the others, and a more thorough investigation is necessary to assess this point.
588 Up to now DUI was identified in only 3 Veneridae species: *Cyclina sinensis*, *R. philippinarum*,
589 and *Meretrix lamarckii* (Gusman et al., 2016). The status of Paphia is still unknown, and in
590 future works it would be interesting to investigate more Heterodonta species to understand better
591 the distribution of DUI in this derived group of bivalves.
592

593 **Acknowledgements**
594 We would like to thank Edoardo Turolla (Istituto Delta Ecologia Applicata, Ferrara, Italy) for
595 providing the specimens, and Massimo Milan for bibliographic suggestions. We also gratefully
596 thank the Editor Tim Collins, and the reviewers Carlos Saavedra, Shallee Page, and one
597 anonymous colleague for their comments and suggestions.

598 **References**

599 Alikhan NF., Petty NK., Ben Zakour NL., Beatson SA. 2011. BLAST Ring Image Generator
600 (BRIG): simple prokaryote genome comparisons. *BMC genomics* 12:402.
601 Arias-Pérez A., Cordero D., Borrell Y., Sánchez JA., Blanco G., Freire R., Insua A.,
602 Saavedra C. 2016. Assessing the geographic scale of genetic population management with
603 microsatellites and introns in the clam Ruditapes decussatus. Ecology and Evolution 15:3380-
604 3404.
605 Attwood TK., Bradley P., Flower DR., Gaulton A., Maudling N., Mitchell AL., Moulton G.,
606 Nordle A., Paine K., Taylor P., Uddin A., Zygouri C. 2003. PRINTS and its automatic
607 supplement, prePRINTS. *Nucleic acids research* 31:400–402.
608 Bailey TL., Boden M., Buske FA., Frith M., Grant CE., Clementi L., Ren J., Li WW., Noble WS.
609 2009. MEME SUITE: tools for motif discovery and searching. *Nucleic acids research*
610 37:W202–8.
611 Bernt M., Donath A., Jühling F., Externbrink F., Florentz C., Fritzsch G., Pütz J., Middendorf
612 M., Stadler PF. 2013. MITOS: improved de novo metazoan mitochondrial genome
613 annotation. *Molecular phylogenetics and evolution* 69:313–319.
614 Breton S., Milani L., Ghiselli F., Guerra D., Stewart DT., Passamonti M. 2014. A resourceful
615 genome: updating the functional repertoire and evolutionary role of animal mitochondrial
616 DNAs. *Trends in genetics: TIG* 30:555–564.
617 Breton S., Stewart DT., Hoeh WR. 2010. Characterization of a mitochondrial ORF from the
618 gender-associated mtDNAs of *Mytilus spp*. (Bivalvia: Mytilidae): identification of the
619 "missing" ATPase 8 gene. *Marine genomics* 3:11–18.
620 Breton S., Stewart DT., Shepardson S., Trdan RJ., Bogan AE., Chapman EG., Ruminas AJ.,

621 Piontkivska H., Hoeh WR. 2011. Novel protein genes in animal mtDNA: a new sex
622 determination system in freshwater mussels (Bivalvia: Unionoida)? *Molecular biology and*
623 *evolution* 28:1645–1659.
624 Broughton RE., Dowling TE. 1994. Length variation in mitochondrial DNA of the minnow
625 *Cyprinella spiloptera*. *Genetics* 138:179–190.
626 Buroker NE., Brown JR., Gilbert TA., O'Hara PJ., Beckenbach AT., Thomas WK., Smith MJ.
627 1990. Length heteroplasmy of sturgeon mitochondrial DNA: an illegitimate elongation
628 model. *Genetics* 124:157–163.
629 Buske FA., Bodén M., Bauer DC., Bailey TL. 2010. Assigning roles to DNA regulatory motifs
630 using comparative genomics. *Bioinformatics* 26:860–866.
631 Cao L., Kenchington E., Zouros E., Rodakis GC. 2004. Evidence that the large noncoding
632 sequence is the main control region of maternally and paternally transmitted mitochondrial
633 genomes of the marine mussel (*Mytilus spp*.). *Genetics* 167:835–850.
634 Capella-Gutiérrez S., Silla-Martinez JM., Gabaldón T. 2009. trimAl: a tool for automated
635 alignment trimming in large-scale phylogenetic analyses. *Bioinformatics* 25:1972–1973.
636 Chamary JV., Parmley JL., Hurst LD. 2006. Hearing silence: non-neutral evolution at
637 synonymous sites in mammals. *Nature reviews. Genetics* 7:98–108.
638 Cordero D., Delgado M., Liu B., Ruesink J., Saavedra C. 2017. Population genetics of the
639 Manila clam (*Ruditapes philippinarum*) introduced in North America and Europe. *Scientific*
640 *reports* 7:39745.
641 Cordero D., Peña JB., Saavedra C. 2014. Phylogeographic analysis of introns and mitochondrial
642 DNA in the clam *Ruditapes decussatus* uncovers the effects of Pleistocene glaciations and
643 endogenous barriers to gene flow. *Molecular phylogenetics and evolution* 71:274–287.

644 Crick FHC. 1966. Codon—anticodon pairing: The wobble hypothesis. *Journal of molecular*
645 *biology* 19:548–555.
646 Darty K., Denise A., Ponty Y. 2009. VARNA: Interactive drawing and editing of the RNA
647 secondary structure. *Bioinformatics* 25:1974–1975.
648 DePristo MA., Banks E., Poplin R., Garimella KV., Maguire JR., Hartl C., Philippakis AA., del
649 Angel G., Rivas MA., Hanna M., McKenna A., Fennell TJ., Kernytsky AM., Sivachenko
650 AY., Cibulskis K., Gabriel SB., Altshuler D., Daly MJ. 2011. A framework for variation
651 discovery and genotyping using next-generation DNA sequencing data. *Nature genetics*
652 43:491–498.
653 Diz AP., Dudley E., Skibinski DOF. 2012. Identification and characterisation of highly
654 expressed proteins in sperm cells of the marine mussel *Mytilus edulis*. *Proteomics*. DOI:
655 10.1002/pmic.201100500.
656 Dreyer H., Steiner G. 2006. The complete sequences and gene organisation of the mitochondrial
657 genomes of the heterodont bivalves *Acanthocardia tuberculata* and *Hiatella arctica*—and
658 the first record for a putative Atpase subunit 8 gene in marine bivalves. *Frontiers in zoology*
659 3:13.
660 Finn RD., Coggill P., Eberhardt RY., Eddy SR., Mistry J., Mitchell AL., Potter SC., Punta M.,
661 Qureshi M., Sangrador-Vegas A., Salazar GA., Tate J., Bateman A. 2016. The Pfam protein
662 families database: towards a more sustainable future. *Nucleic acids research* 44:D279–85.
663 Ghiselli F., Milani L., Chang PL., Hedgecock D., Davis JP., Nuzhdin SV., Passamonti M. 2012.
664 De Novo assembly of the Manila clam *Ruditapes philippinarum* transcriptome provides
665 new insights into expression bias, mitochondrial doubly uniparental inheritance and sex
666 determination. *Molecular biology and evolution* 29:771–786.

667 Ghiselli F., Milani L., Guerra D., Chang PL., Breton S., Nuzhdin SV., Passamonti M. 2013.
668 Structure, transcription, and variability of metazoan mitochondrial genome: perspectives
669 from an unusual mitochondrial inheritance system. *Genome biology and evolution* 5:1535–
670 1554.
671 Ghiselli F., Milani L., Passamonti M. 2011. Strict sex-specific mtDNA segregation in the germ
672 line of the DUI species *Venerupis philippinarum* (Bivalvia: Veneridae). *Molecular biology*
673 *and evolution* 28:949–961.
674 Gissi C., Iannelli F., Pesole G. 2008. Evolution of the mitochondrial genome of Metazoa as
675 exemplified by comparison of congeneric species. *Heredity* 101:301–320.
676 Gosling EM. 2003. *Bivalve molluscs*. Wiley Online Library.
677 Gott JM., Emeson RB. 2000. Functions and mechanisms of RNA editing. *Annual Review of*
678 *Genetics*. 34:499–531.
679 Gruber AR., Lorenz R., Bernhart SH., Neuböck R., Hofacker IL. 2008. The Vienna RNA
680 websuite. *Nucleic acids research* 36:W70–4.
681 Guerra D., Ghiselli F., Passamonti M. 2014. The largest unassigned regions of the male- and
682 female-transmitted mitochondrial DNAs in *Musculista senhousia* (Bivalvia Mytilidae).
683 *Gene* 536:316–325.
684 Gusman A., Lecomte S., Stewart DT., Passamonti M., Breton S. 2016. Pursuing the quest for
685 better understanding the taxonomic distribution of the system of doubly uniparental
686 inheritance of mtDNA. *PeerJ* 4:e2760.
687 Hayasaka K., Ishida T., Horai S. 1991. Heteroplasmy and polymorphism in the major noncoding
688 region of mitochondrial DNA in Japanese monkeys: association with tandemly repeated
689 sequences. *Molecular biology and evolution* 8:399–415.

690 He Z., Zhang H., Gao S., Lercher MJ., Chen W-H., Hu S. 2016. Evolview v2: an online
691 visualization and management tool for customized and annotated phylogenetic trees.
692 *Nucleic acids research* 44:W236–41.
693 Hoeh WR., Stewart DT., Saavedra C., Sutherland BW., Zouros E. 1997. Phylogenetic evidence
694 for role-reversals of gender-associated mitochondrial DNA in Mytilus (Bivalvia: Mytilidae).
695 *Molecular Biology and Evolution* 14:959–967.
696 Huang X., Madan A. 1999. CAP3: A DNA sequence assembly program. *Genome research*
697 9:868–877.
698 Jones P., Binns D., Chang H-YY., Fraser M., Li W., McAnulla C., McWilliam H., Maslen J.,
699 Mitchell A., Nuka G., et al. 2014. InterProScan 5: genome-scale protein function
700 classification. *Bioinformatics* 30:1236–1240.
701 Ju YS., Kim J-I., Kim S., Hong D., Park H., Shin J-Y., Lee S., Lee W-C., Kim S., Yu S-B., et al.
702 2011. Extensive genomic and transcriptional diversity identified through massively parallel
703 DNA and RNA sequencing of eighteen Korean individuals. *Nature Genetics*. 43:745–752.
704 King JL., LaRue BL., Novroski NM., Stoljarova M., Seo SB., Zeng X., Warshauer DH., Davis
705 CP., Parson W., Sajantila A., et al. 2014. High-quality and high-throughput massively
706 parallel sequencing of the human mitochondrial genome using the Illumina MiSeq.
707 *Forensic Science International: Genetics*. 12:128–135.
708 La Roche J., Snyder M., Cook DI., Fuller K., Zouros E. 1990. Molecular characterization of a
709 repeat element causing large-scale size variation in the mitochondrial DNA of the sea
710 scallop *Placopecten magellanicus*. *Molecular biology and evolution* 7:45–64.
711 Laslett D., Canback B. 2008. ARWEN: a program to detect tRNA genes in metazoan
712 mitochondrial nucleotide sequences. *Bioinformatics* 24:172–175.

713 Lavrov DV., Pett W. 2016. Animal Mitochondrial DNA as We Do Not Know It: mt-Genome
714 Organization and Evolution in Nonbilaterian Lineages. *Genome biology and evolution*
715 8:2896–2913.
716 Leite RB., Milan M., Coppe A., Bortoluzzi S., dos Anjos A., Reinhardt R., Saavedra C.,
717 Patarnello T., Cancela ML., Bargelloni L. 2013. mRNA-Seq and microarray development
718 for the Grooved Carpet shell clam, *Ruditapes decussatus*: a functional approach to unravel
719 host-parasite interaction. *BMC genomics* 14:741.
720 Liscovitch-Brauer N., Alon S., Porath HT., Elstein B., Unger R., Ziv T., Admon A., Levanon
721 EY., Rosenthal JJC., Eisenberg E. 2017. Trade-off between Transcriptome Plasticity and
722 Genome Evolution in Cephalopods. *Cell* 169:191–202.e11.
723 Lubośny M., Przyłucka A., Sańko TJ., Śmietanka B., Rosenfeld S., Burzyński A. 2017/2. Next
724 generation sequencing of gonadal transcriptome suggests standard maternal inheritance of
725 mitochondrial DNA in *Eurhomalea rufa* (Veneridae). *Marine genomics* 31:21–23.
726 McKenna A., Hanna M., Banks E., Sivachenko A., Cibulskis K., Kernytsky A., Garimella K.,
727 Altshuler D., Gabriel S., Daly M., DePristo MA. 2010. The Genome Analysis Toolkit: a
728 MapReduce framework for analyzing next-generation DNA sequencing data. *Genome*
729 *research* 20:1297–1303.
730 Milani L., Ghiselli F. 2015. Mitochondrial activity in gametes and transmission of viable
731 mtDNA. *Biology direct* 10:22.
732 Milani L., Ghiselli F., Guerra D., Breton S., Passamonti M. 2013. A comparative analysis of
733 mitochondrial ORFans: new clues on their origin and role in species with doubly
734 uniparental inheritance of mitochondria. *Genome biology and evolution* 5:1408–1434.
735 Milani L., Ghiselli F., Iannello M., Passamonti M. 2014a. Evidence for somatic transcription of

736 male-transmitted mitochondrial genome in the DUI species *Ruditapes philippinarum*
737 (Bivalvia: Veneridae). *Current genetics* 60:163–173.
738 Milani L., Ghiselli F., Maurizii MG., Nuzhdin SV., Passamonti M. 2014b. Paternally transmitted
739 mitochondria express a new gene of potential viral origin. *Genome biology and evolution*
740 6:391–405.
741 Milani L., Ghiselli F., Passamonti M. 2016. Mitochondrial selfish elements and the evolution of
742 biological novelties. *Current zoology* 62:687–697.
743 Milbury CA., Lee JC., Cannone JJ., Gaffney PM., Gutell RR. 2010. Fragmentation of the large
744 subunit ribosomal RNA gene in oyster mitochondrial genomes. *BMC genomics* 11:485.
745 Mitchell A., Guerra D., Stewart D., Breton S. 2016. In silico analyses of mitochondrial ORFans
746 in freshwater mussels (Bivalvia: Unionoida) provide a framework for future studies of their
747 origin and function. *BMC Genomics* 17:597.
748 Mortazavi A., Williams BA., McCue K., Schaeffer L., Wold B. 2008. Mapping and quantifying
749 mammalian transcriptomes by RNA-Seq. *Nature methods* 5:621–628.
750 Namiki T., Hachiya T., Tanaka H., Sakakibara Y. 2012. MetaVelvet: an extension of
751 Velvet assembler to de novo metagenome assembly from short sequence reads.
752 *Nucleic Acids Research*. 40:e155.
753 Ojala D., Montoya J., Attardi G. 1981. tRNA punctuation model of RNA processing in
754 human mitochondria. *Nature*. 290:470–4.
755 Passamonti M., Ghiselli F. 2009. Doubly uniparental inheritance: two mitochondrial genomes,
756 one precious model for organelle DNA inheritance and evolution. *DNA and cell biology*
757 28:79–89.
758 Passamonti M., Mantovani B., Scali V. 1997. Allozymic characterization and genetic

759 relationships among four species of Tapetinae (Bivalvia, Veneridae). *Italian journal of*
760 *zoology* 64:117–124.
761 Passamonti M., Mantovani B., Scali V. 1998. Characterization of a highly repeated DNA family
762 in tapetinae species (mollusca bivalvia: veneridae). *Zoological science* 15:599–605.
763 Passamonti M., Mantovani B., Scali V. 1999. Allozymic analysis of some Mediterranean
764 Veneridae (Mollusca: Bivalvia): preliminary notes on taxonomy and systematics of the
765 family. *Journal of the Marine Biological Association of the United Kingdom. Marine*
766 *Biological Association of the United Kingdom* 79:899–906.
767 Passamonti M., Ricci A., Milani L., Ghiselli F. 2011. Mitochondrial genomes and Doubly
768 Uniparental Inheritance: new insights from *Musculista senhousia* sex-linked mitochondrial
769 DNAs (Bivalvia Mytilidae). *BMC genomics* 12:442.
770 Pesole G., Allen JF., Lane N., Martin W., Rand DM., Schatz G., Saccone C. 2012. The neglected
771 genome. *EMBO reports* 13:473–474.
772 Plazzi F., Puccio G., Passamonti M. 2016. Comparative Large-Scale Mitogenomics Evidences
773 Clade-Specific Evolutionary Trends in Mitochondrial DNAs of Bivalvia. *Genome biology*
774 *and evolution* 8:2544–2564.
775 Pozzi A., Plazzi F., Milani L., Ghiselli F., Passamonti M. 2017. SmithRNAs: could mitochondria
776 "bend" nuclear regulation? *Molecular biology and evolution*. DOI:
777 10.1093/molbev/msx140.
778 Rozen S., Skaletsky H. 2000. Primer3 on the WWW for general users and for biologist
779 programmers. *Methods in molecular biology* 132:365–386.
780 Scheffler IE. 2008. *Mitochondria*. Hoboken, N.J.: Wiley.
781 Scheibye-Alsing K., Cirera S., Gilchrist MJ., Fredholm M., Gorodkin J. 2007. EST analysis on

782 pig mitochondria reveal novel expression differences between developmental and adult
783 tissues. *BMC genomics* 8:367.
784 Serb JM., Lydeard C. 2003. Complete mtDNA sequence of the North American freshwater
785 mussel, *Lampsilis ornata* (Unionidae): an examination of the evolution and phylogenetic
786 utility of mitochondrial genome organization in Bivalvia (Mollusca). *Molecular biology and*
787 *evolution* 20:1854–1866.
788 Sievers F., Wilm A., Dineen D., Gibson TJ., Karplus K., Li W., Lopez R., McWilliam H.,
789 Remmert M., Söding J., Thompson JD., Higgins DG. 2011. Fast, scalable generation of
790 high-quality protein multiple sequence alignments using Clustal Omega. *Molecular systems*
791 *biology* 7:539.
792 Skibinski DO., Gallagher C., Beynon CM. 1994a. Mitochondrial DNA inheritance. *Nature*
793 368:817–818.
794 Skibinski DO., Gallagher C., Beynon CM. 1994b. Sex-limited mitochondrial DNA transmission
795 in the marine mussel *Mytilus edulis*. *Genetics* 138:801–809.
796 Smith DR. 2013. RNA-Seq data: a goldmine for organelle research. *Briefings in functional*
797 *genomics* 12:454–456.
798 de Sousa JT., Milan M., Bargelloni L., Pauletto M., Matias D., Joaquim S., Matias AM., Quillien
799 V., Leitão A., Huvet A. 2014. A microarray-based analysis of gametogenesis in two
800 Portuguese populations of the European clam *Ruditapes decussatus*. *PloS one* 9:e92202.
801 Stamatakis A. 2014. RAxML version 8: a tool for phylogenetic analysis and post-analysis of
802 large phylogenies. *Bioinformatics* 30:1312–1313.
803 Stothard P. 2000. The sequence manipulation suite: JavaScript programs for analyzing and
804 formatting protein and DNA sequences. *BioTechniques* 28:1102, 1104.

805 Sullivan MJ., Petty NK., Beatson SA. 2011. Easyfig: a genome comparison visualizer.
806 *Bioinformatics* 27:1009–1010.
807 Tamura K., Stecher G., Peterson D., Filipski A., Kumar S. 2013. MEGA6: Molecular
808 Evolutionary Genetics Analysis version 6.0. *Molecular biology and evolution* 30:2725–
809 2729.
810 Tan MH., Gan HM., Schultz MB., Austin CM. 2015. MitoPhAST, a new automated
811 mitogenomic phylogeny tool in the post-genomic era with a case study of 89 decapod
812 mitogenomes including eight new freshwater crayfish mitogenomes. *Molecular*
813 *phylogenetics and evolution*. DOI: 10.1016/j.ympev.2015.02.009.
814 Theologidis I., Fodelianakis S., Gaspar MB., Zouros E. 2008. Doubly uniparental inheritance
815 (DUI) of mitochondrial DNA in *Donax trunculus* (Bivalvia: Donacidae) and the problem of
816 its sporadic detection in Bivalvia. *Evolution; international journal of organic evolution*
817 62:959–970.
818 Tritt A., Eisen JA., Facciotti MT., Darling AE. 2012. An integrated pipeline for de novo
819 assembly of microbial genomes. *PloS one* 7:e42304.
820 Wheeler DL., Church DM., Federhen S., Lash AE., Madden TL., Pontius JU., Schuler GD.,
821 Schriml LM., Sequeira E., Tatusova TA., Wagner L. 2005. Database resources of the
822 National Center for Biotechnology. *Nucleic Acid Research* 33:D39–D45.
823 Yu H., Li Q. 2011. Mutation and selection on the wobble nucleotide in tRNA anticodons in
824 marine bivalve mitochondrial genomes. PLoS One 6:e16147.
825 Yuan Y., Li Q., Yu H., Kong L. 2012. The complete mitochondrial genomes of six heterodont
826 bivalves (Tellinoidea and Solenoidea): variable gene arrangements and phylogenetic
827 implications. *PloS one* 7:e32353.

828 Yuan S., Xia Y., Zheng Y., Zeng X. 2016. Next-generation sequencing of mixed genomic DNA
829 allows efficient assembly of rearranged mitochondrial genomes in *Amolops chunganensis*
830 and *Quasipaa boulengeri*. *PeerJ* 4:e2786.
831 Zouros E. 2013. Biparental Inheritance Through Uniparental Transmission: The Doubly
832 Uniparental Inheritance (DUI) of Mitochondrial DNA. *Evolutionary biology* 40:1–31.
833 Zouros E., Ball AO., Saavedra C., Freeman KR. 1994a. Mitochondrial DNA inheritance. *Nature*
834 368:818.
835 Zouros E., Oberhauser Ball A., Saavedra C., Freeman KR. 1994b. An unusual type of
836 mitochondrial DNA inheritance in the blue mussel Mytilus. *Proceedings of the National*
837 *Academy of Sciences of the United States of America* 91:7463–7467.

Figure 1(on next page)

R. decussatus mtDNA gene arrangement

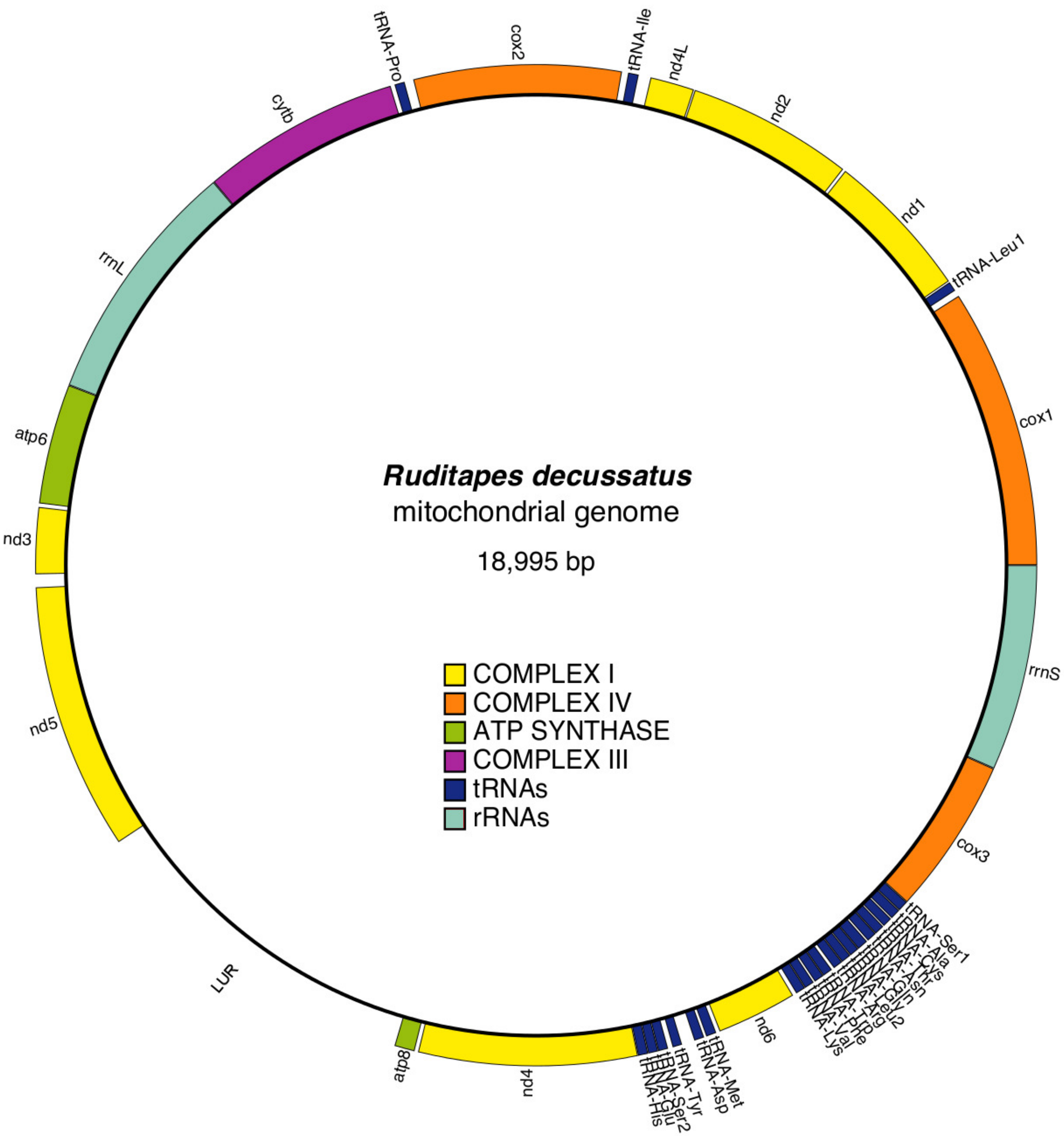
Ruditapes decussatus
mitochondrial genome
18,995 bp
COMPLEX I
COMPLEX IV
ATP SYNTHASE
COMPLEX III
tRNAs
rRNAs
tRNA-Pro
cox2
tRNA-Ile
nd4L
nd2
nd1
tRNA-Leu1
cox1
rrnS
cox3
tRNA-Ser1
tRNA-Ala
tRNA-Cys
tRNA-Thr
tRNA-Asn
tRNA-Gln
tRNA-Leu2
tRNA-Arg
tRNA-Phe
tRNA-Val
tRNA-Lys
nd6
tRNA-Met
tRNA-Asp
tRNA-Tyr
tRNA-Ser2
tRNA-Glu
tRNA-His
nd4
atp8
LUR
nd5
nd3
atp6
rrnL
cytb

Figure 2(on next page)

Principal features of the Largest Unassigned Region (LUR)

A: map of the lUR; B: DNA secondary structure predicted in the repeat region (boxed in A); C: Logos of the two DNA motifs found in the LUR.

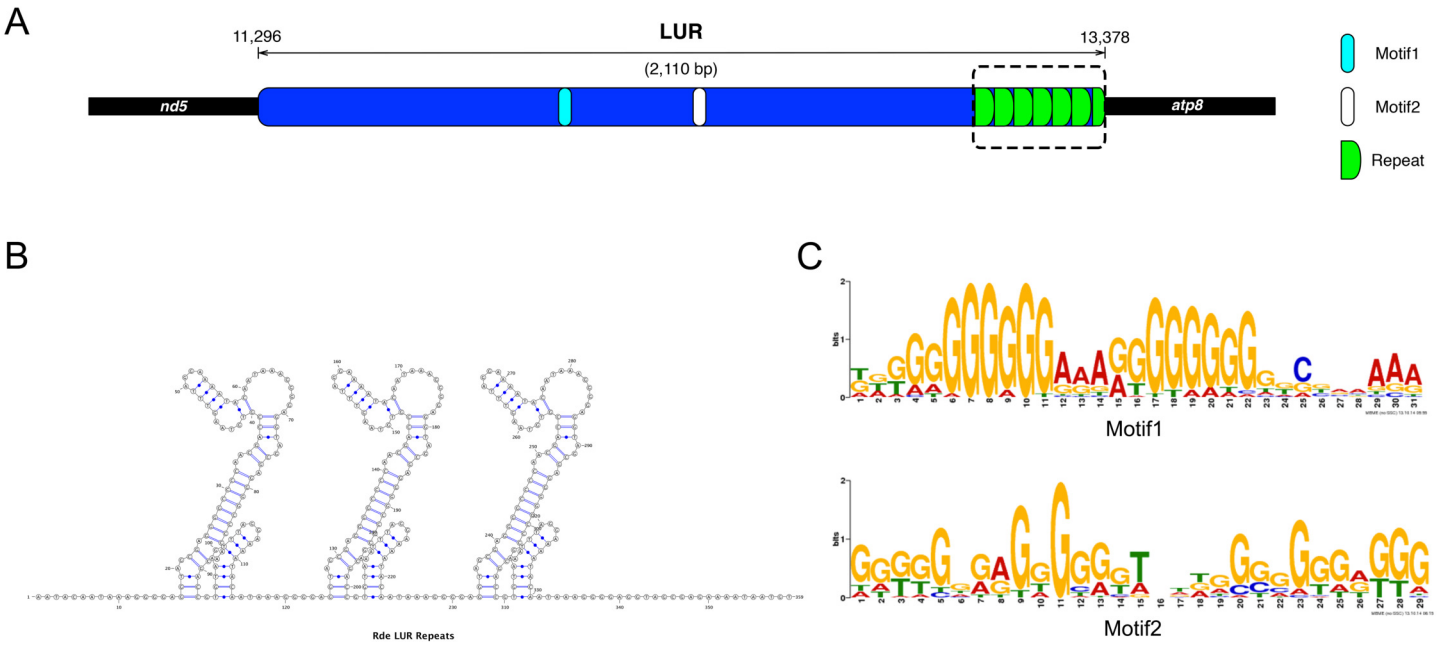
A
11,296
LUR
13,378
(2,110 bp)
nd5
atp8
Motif1
Motif2
Repeat
B
Rde LUR Repeats
C
Motif1
Motif2

Figure 3(on next page)

BLASTN comparison of *R. decussatus* and other Veneridae

R. decussatus mtDNA map (external gray circle), and BLASTN identity (colored inner circles) with complete mtDNAs of other 10 venerid species (see list in Supplementary Table 3).

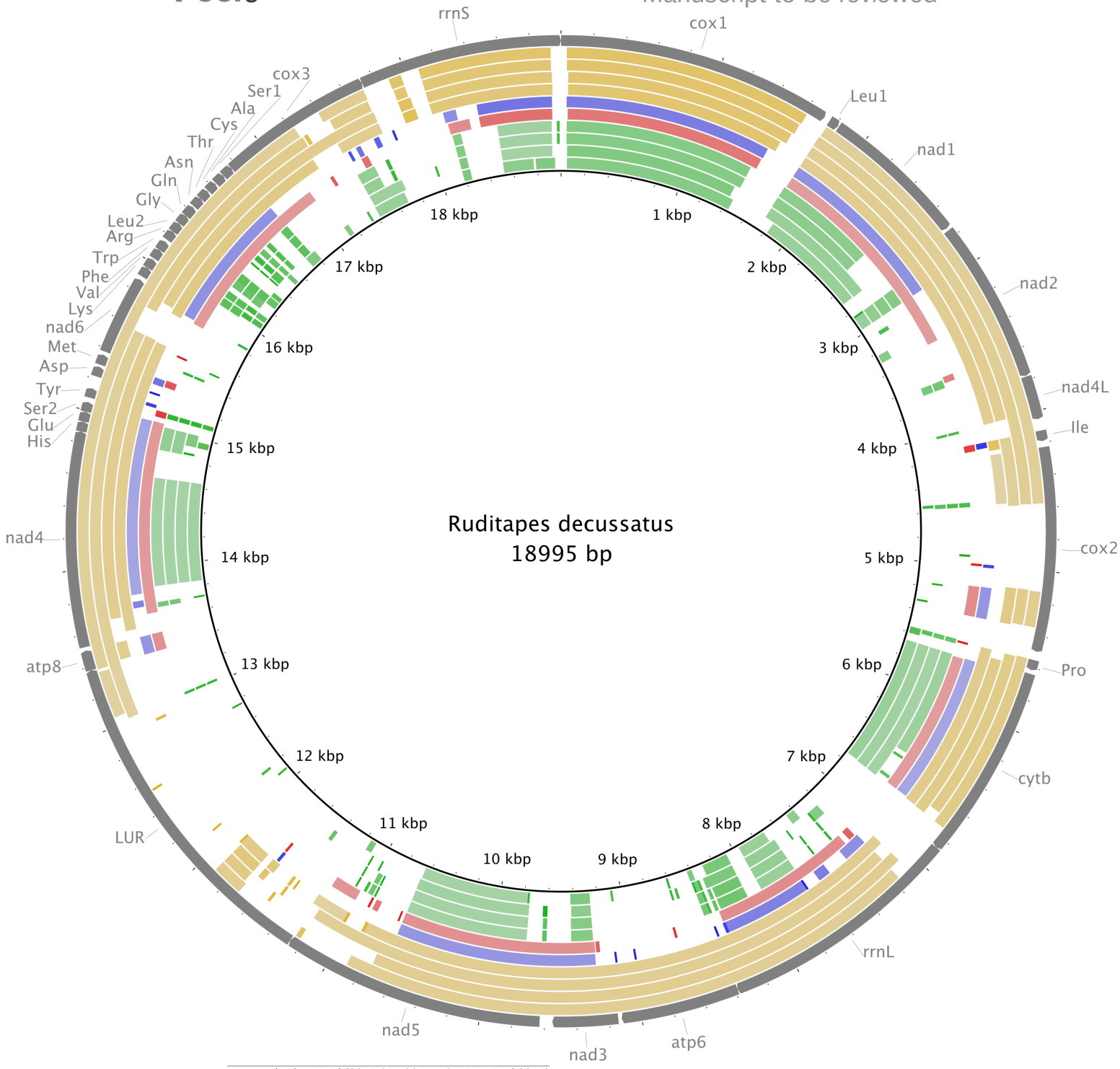

Meretrix lamarckii
100% identity
70% identity
50% identity
Meretrix lusoria
100% identity
70% identity
50% identity
Meretrix meretrix
100% identity
70% identity
50% identity
Meretrix petechialis
100% identity
70% identity
50% identity
Ruditapes philippinarum F-Type
100% identity
70% identity
50% identity
Ruditapes philippinarum M-Type
100% identity
70% identity
50% identity
Paphia amabilis
100% identity
70% identity
50% identity
Paphia euglypta
100% identity
70% identity
50% identity
Paphia textile
100% identity
70% identity
50% identity
Paphia undulata
100% identity
70% identity
50% identity
Annotation

38 of the 38 labels are shown.

Figure 4(on next page)

Maximum Likelihood (ML) tree of Veneridae obtained with all mitochondrial coding genes.

ML tree obtained with the MitoPhast pipeline; the complete input and output of this analysis is available on figshare (https://doi.org/10.6084/m9.figshare.4970762.v1).

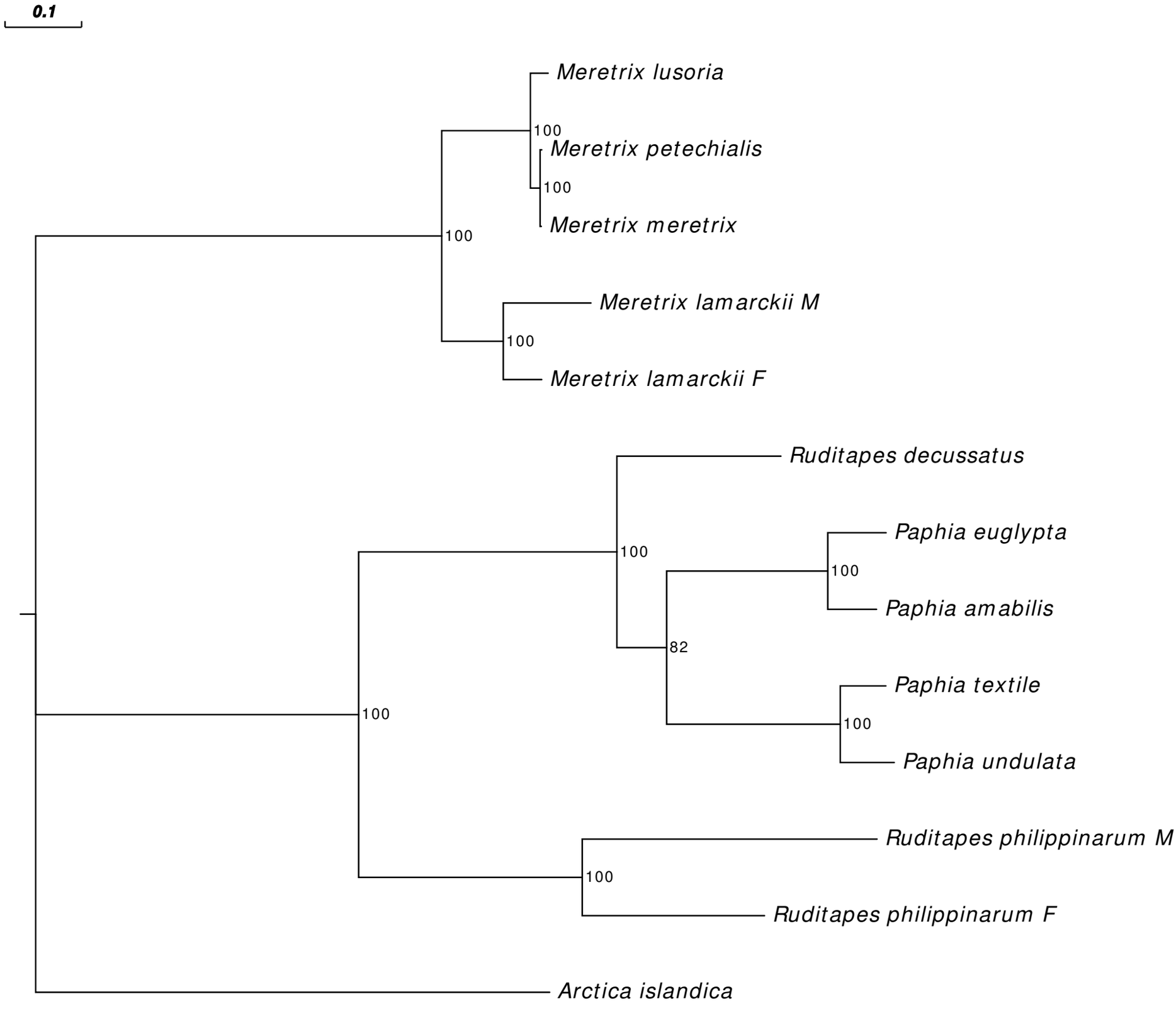
0.1
Meretrix lusoria
100
Meretrix petechialis
100
Meretrix meretrix
100
Meretrix lamarckii M
100
Meretrix lamarckii F
Ruditapes decussatus
100
Paphia euglypta
100
Paphia amabilis
82
Paphia textile
100
Paphia undulata
100
Ruditapes philippinarum M
100
Ruditapes philippinarum F
Arctica islandica

Figure 5(on next page)

Comparison of gene order in venerid mtDNAs

Variation in gene order between *R. decussatus* and *P. euglypta* (Figure 5A), *M. lamarckii* F-type (Figure 5B), *R. philippinarum* F-type (Figure 5C), and among all the 4 species (Figure 5D).

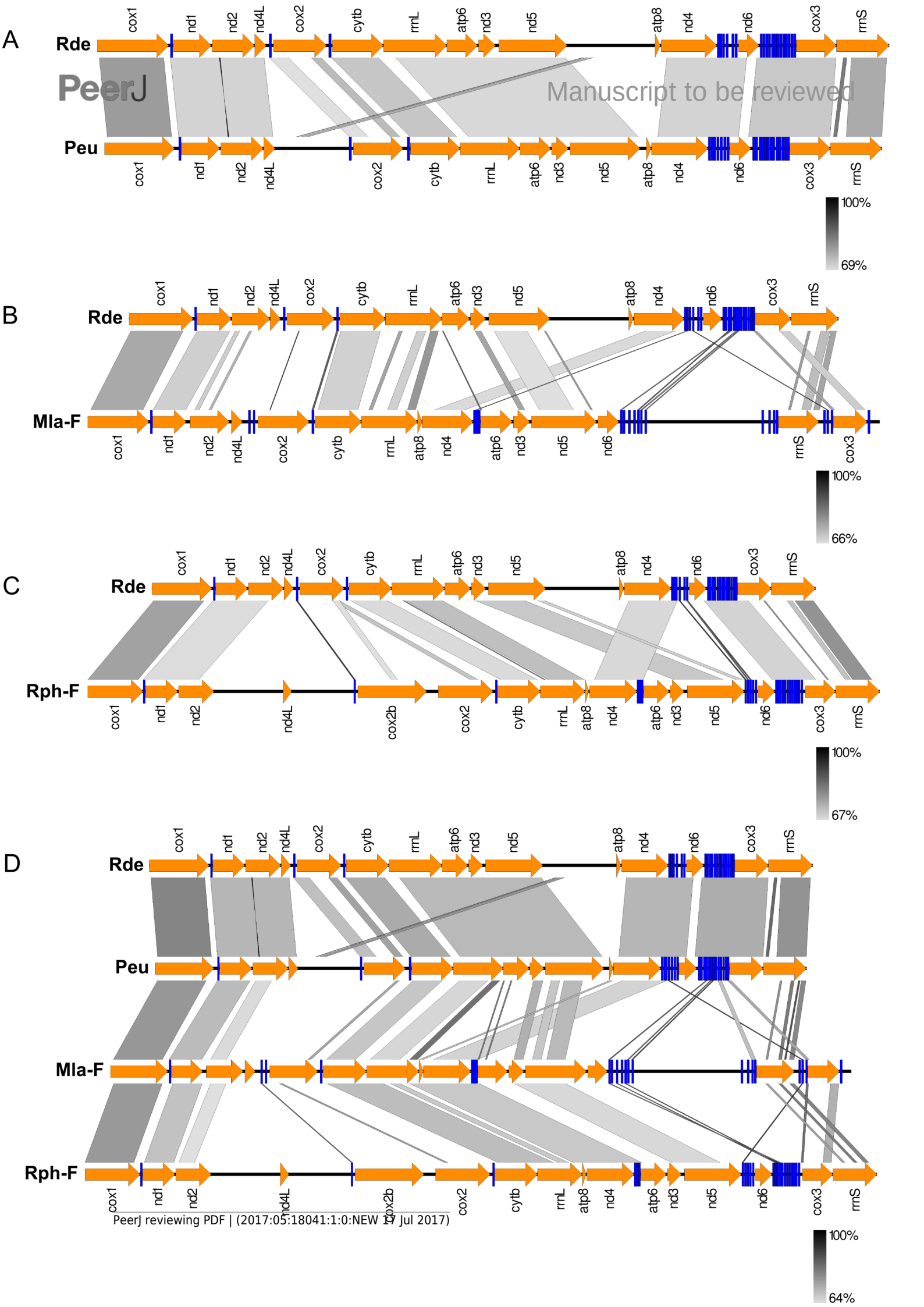

Table 1(on next page)

Features of the contigs obtained by *de novo* assembly of mtDNA.

1 **Table 1** Features of the contigs obtained by *de novo* assembly of mtDNA.

2

Contig	Length	Gene content	Poly-A	Notes
1	6794	*atp6_nd3_nd5_cox1_tRNA-Leu1_nd1_nd2_nd4L*	Yes	Chimeric assembly. The contiguity between *nd5* and *cox1* is an artifact
2	1884	*rrnS_cox3*	No	-
3	1288	*atp6_nd3*	Yes	-
4	1663	*cox3*	?	The contig ends with just 8 As
5	1934	*atp8_nd4_tRNA-His_tRNA-Glu_tRNA-Ser2_tRNA-Tyr*	No	-
6	1831	*atp8_nd4_tRNA-His*	Yes	-
7	5478	*cox2_tRNA-Ile_nd4L_nd2_nd1_tRNA-Leu1_cox1*	Yes	There is a polyadenylation signal (56 As) after the *cox2* gene
8	2879	*cytb_rrnL*	No	-
9	952	*nd6_tRNA-Lys_tRNA-Val_tRNA-Phe_tRNA-Trp_tRNA-Arg_tRNA-Leu2*	No	-

Table 2(on next page)

MtDNA gene arrangement of *R. decussatus*.

The anticodon of tRNAs are reported in the 5’-3’ direction.

Table 2 MtDNA gene arrangement of *R. decussatus*. The anticodon of tRNAs are reported in the 5'-3' direction.

Name	Type	Start	Stop	Length (bp)	Start	Stop	Anticodon
cox1	Coding	1	1,716	1,716	ATA	TAG	
tRNA-Leu1	tRNA	1,754	1,815	62			TAG
nd1	Coding	1,822	2,739	918	ATA	TAA	
nd2	Coding	2,755	3,774	1,020	ATG	TAG	
nd4l	Coding	3,780	4,052	273	ATA	TAG	
tRNA-Ile	tRNA	4,125	4,190	66			GAT
cox2	Coding	4,228	5,499	1,272	ATA	TAG	
tRNA-Pro	tRNA	5,553	5,616	64			TGG
cytb	Coding	5,641	6,864	1,224	ATA	TAG	
rrnL	rRNA	6,865	8,385	1,521			
atp6	Coding	8,386	9,123	738	ATG	TAA	
nd3	Coding	9,145	9,552	408	ATG	TAA	
nd5	Coding	9,631	11,268	1,638	ATG	TAG	
atp8	Coding	13,379	13,504	126	ATA	TAA	
nd4	Coding	13,526	14,865	1,340	ATA	TA*	
tRNA-His	tRNA	14,866	14,928	63			GTG
tRNA-Glu	tRNA	14,929	14,990	62			TTC
tRNA-Ser2	tRNA	14,991	15,052	62			TGA
tRNA-Tyr	tRNA	15,081	15,140	60			GTA
tRNA-Asp	tRNA	15,218	15,280	63			GTC
tRNA-Met	tRNA	15,294	15,358	65			CAT
nd6	Coding	15,380	15,874	495	ATG	TAA	
tRNA-Lys	tRNA	15,897	15,959	63			TTT
tRNA-Val	tRNA	15,960	16,021	62			TAC
tRNA-Phe	tRNA	16,030	16,092	63			GAA
tRNA-Trp	tRNA	16,093	16,155	63			TCA
tRNA-Arg	tRNA	16,171	16,232	62			TCG
tRNA-Leu2	tRNA	16,233	16,295	63			TAA
tRNA-Gly	tRNA	16,297	16,358	62			TCC
tRNA-Gln	tRNA	16,359	16,427	69			TTG
tRNA-Asn	tRNA	16,435	16,497	63			GTT
tRNA-Thr	tRNA	16,498	16,560	63			TGT
tRNA-Cys	tRNA	16,565	16,626	62			GCA
tRNA-Ala	tRNA	16,632	16,696	65			TGC
tRNA-Ser1	tRNA	16,698	16,764	67			TCT
cox3	Coding	16,765	17,730	966	ATG	TAA	
rrnS	rRNA	17,731	18,995	1,265			

Table 3(on next page)

Unassigned Regions (URs)

Table 3 Unassigned Regions (URs)

UR name	Start	Stop	Length (bp)
UR1	1,717	1,753	37
UR2	1,816	1,821	6
UR3	2,740	2,754	15
UR4	3,775	3,779	5
UR5	4,053	4,124	72
UR6	4,191	4,227	37
UR7	5,500	5,552	53
UR8	5,617	5,640	24
UR9	9,124	9,144	21
UR10	9,553	9,630	78
UR11 (LUR)	11,269	13,378	2,110
UR12	13,505	13,525	21
UR13	15,053	15,080	28
UR14	15,141	15,217	77
UR15	15,281	15,293	13
UR16	15,359	15,379	21
UR17	15,875	15,896	22
UR18	16,022	16,029	8
UR19	16,156	16,170	15
UR20	16,296	16,296	1
UR21	16,428	16,434	7
UR22	16,561	16,564	4
UR23	16,627	16,631	5
UR24	16,697	16,697	1

Table 4(on next page)

Nucleotide composition.

URs = Unassigned Regions.

Table 4 Nucleotide composition. URs = Unassigned Regions.

Name	Length (bp)	T %	C %	A %	G %	A+T %	T3 %	C3 %	A3 %	G3 %	A3+T3 %
cox1	1,716	35.8	15.5	25.8	22.9	61.6	39	12.1	28.0	21.3	67.0
nd1	918	38.7	12.5	24.0	24.8	62.7	38	10.1	30.7	21.2	68.7
nd2	1,020	38.3	11.0	24.8	25.9	63.1	35	11.5	29.4	24.4	64.4
nd4l	273	39.9	12.8	25.3	22.0	65.2	34	14.3	30.8	20.9	64.8
cox2	1,272	29.7	14.8	29.1	26.4	58.8	30	15.3	27.4	27.6	57.4
cob	1,224	37.4	17.2	22.7	22.6	60.1	41	14.7	21.8	22.1	62.8
rrnL	1,749	33.2	11.5	32.6	22.6	65.8	33	10.6	33.4	23.0	66.4
atp6	510	42.0	15.7	20.8	21.6	62.8	45	13.5	21.8	20.0	66.8
nd3	408	39.5	11.0	24.8	24.8	64.3	33	11.0	30.1	25.7	63.1
nd5	1,638	37.6	11.7	27.7	23.0	65.3	35	11.0	34.2	19.8	69.2
atp8	126	44.4	11.9	19.0	24.6	63.4	45	4.8	23.8	26.2	68.8
nd4	1,340	38.9	12.9	22.1	26.1	61.0	41	10.8	24.9	23.5	65.9
nd6	495	39.2	12.1	23.0	25.7	62.2	38	13.9	27.9	20.0	65.9
cox3	966	36.9	12.7	24.8	25.6	61.7	39	9.6	28.6	23.0	67.6
rrnS	1,265	32.7	12.3	32.9	22.1	65.6	35	13.5	31.6	19.5	66.6
All coding	14,920	36.3	13.2	26.5	24.0	63.0	37	12.0	28.9	22.4	65.7
All *rRNAs*	3,014	32.9	23.8	32.7	22.3	65.7					
All *tRNAs*	1,394	35.4	12.8	30.2	21.7	65.6					
All URs	2,681	28.2	14.1	34.1	23.6	62.3					
All genic DNA	16,314	36.2	13.2	26.8	23.8	63.0					
All DNA	18,995	35.1	13.3	27.9	23.7	63.0					

Table 5(on next page)

Codon usage.

The codons corresponding to a tRNA present in the mitochondrial genome are underlined and in bold. The highest frequency among synonymous codons is also underlined and in bold. # = number of codons; Frequency = frequency of each codon among synonymous codons; %TOT =frequency of each codon among all the codons.

Table 5 Codon usage. The codons corresponding to a tRNA present in the mitochondrial genome are underlined and in bold. The highest frequency among synonymous codons is also underlined and in bold. # = number of codons; Frequency = frequency of each codon among synonymous codons; %TOT =frequency of each codon among all the codons.

Amino Acid	Codon	#	Frequency	%TOT	Amino Acid	Codon	#	Frequency	%TOT
Ala	GCG	29	0.15	0.73	Pro	CCG	16	0.12	0.40
	GCA	44	0.23	1.11		**CCA**	36	0.27	0.91
	GCT	85	**0.45**	2.14		CCT	58	**0.43**	1.46
	GCC	30	0.16	0.76		CCC	24	0.18	0.61
Cys	TGT	94	**0.76**	2.37	Gln	CAG	25	0.44	0.63
	TGC	30	0.24	0.76		**CAA**	32	**0.56**	0.81
Asp	GAT	54	**0.66**	1.36	Arg	CGG	23	0.31	0.58
	GAC	28	0.34	0.71		**CGA**	21	0.28	0.53
Glu	GAG	87	**0.6**	2.19		CGT	25	**0.33**	0.63
	GAA	58	0.4	1.46		CGC	6	0.08	0.15
Phe	TTT	269	**0.78**	6.78	Ser	AGG	69	0.19	1.74
	TTC	78	0.22	1.97		**AGA**	69	0.19	1.74
Gly	GGG	131	**0.4**	3.30		AGT	55	0.15	1.39
	GGA	61	0.19	1.54		AGC	23	0.06	0.58
	GGT	98	0.3	2.47		TCG	18	0.05	0.45
	GGC	36	0.11	0.91		**TCA**	33	0.09	0.83
His	CAT	37	**0.62**	0.93		TCT	76	**0.21**	1.92
	CAC	23	0.38	0.58		TCC	22	0.06	0.55
Ile	ATT	165	**0.8**	4.16	Thr	ACG	21	0.17	0.53
	ATC	40	0.2	1.01		**ACA**	30	0.24	0.76
Lys	AAG	61	0.41	1.54		ACT	57	**0.46**	1.44
	AAA	87	**0.59**	2.19		ACC	16	0.13	0.40
Leu	TTG	122	0.23	3.08	Val	GTG	113	0.3	2.85
	TTA	210	**0.39**	5.29		**GTA**	121	**0.32**	3.05
	CTG	43	0.08	1.08		GTT	119	0.32	3.00
	CTA	70	0.13	1.76		GTC	23	0.06	0.58
	CTT	75	0.14	1.89	Trp	TGG	58	**0.54**	1.46
	CTC	20	0.04	0.50		**TGA**	49	0.46	1.24
Met	**ATG**	86	0.36	2.17	Tyr	TAT	103	**0.69**	2.60
	ATA	155	**0.64**	3.91		**TAC**	47	0.31	1.18
Asn	AAT	76	**0.66**	1.92	STOP	TAG	34	0.58	0.86
	AAC	39	0.34	0.98		TAA	25	0.42	0.63

7
8
9
10

Table 6(on next page)

LUR length and number of repeats in the 13 female samples analyzed.

F3 and F17 are heteroplasmic with LURs of different length.

Table 6 LUR length and number of repeats in the 13 female samples analyzed. F3 and F17 are heteroplasmic with LURs of different length.

Specimen	Length (bp)	Number of Repeats	GenBank Acc. No.
F3	2,100 - 3,500	6.5 - 25	MF055702
F5	5,000	45	MF055703
F7	3,500	25	MF055704
F9	3,500	25	MF055705
F10	3,000	20	MF055706
F11	3,000	20	MF055707
F13	3,500	25	MF055708
F15	3,000	20	MF055709
F16	3,500	25	MF055710
F17	2,500 - 3,500	8 - 25	MF055711
F19	3,500	25	MF055712
F20	2,500	8	MF055713
F21	2,100	6.5	MF055714

Table 7 (on next page)

Sequence Polymorphism (SP): SNPs and small indels called by GATK.

CDS = coding sequences; Whole mtDNA = polymorphism in the whole mitochondrial genome; the number in brackets the bottom of the table represent private SPs (e.g.: there are 23 female specific SPs in the whole mtDNA and 9 female specific SPs in CDS); p-value = significance of the Fisher's exact test on number of SPs between sexes (i.e.: all males vs females, males except mRDI01 vs females).

Table 7 Sequence Polymorphism (SP): SNPs and small indels called by GATK. CDS = coding sequences; Whole mtDNA = polymorphism in the whole mitochondrial genome; the number in brackets the bottom of the table represent private SPs (e.g.: there are 23 female specific SPs in the whole mtDNA and 9 female specific SPs in CDS); p-value = significance of the Fisher's exact test on number of SPs between sexes (i.e.: all males vs females, males except mRDI01 vs females).

FEATURE	VALUE	MIN	MEDIAN	MEAN	MAX
Depth (all SPs)	-	6	1,357	1,521	3,880
Phred Score (all SPs)	-	3.30E+01	5.76E+03	4.18E+07	2.15E+09
Depth (SPs in CDS)	-	222	2,038	2,150	3,880
Phred Score (SPs in CDS)	-	1.18E+02	1.01E+04	4.45E+07	2.15E+09
Total number of SPs	257	-	-	-	-
Number of mRDI01 private SPs	151 (58.7% of the total)	-	-	-	-
Number of SPs in CDS	145 (56.4% of the total)	-	-	-	-
Number of mRDI01 private SPs in CDS	103 (71% of the SNPs in CDS)	-	-	-	-
Number of SPs in CDS (excluding mRDI01)	42	-	-	-	-
Frequency of SPs in CDS	0.0097 (~ 1 every 103bp)	-	-	-	-
Frequency of SPs in CDS (excluding mRDI01)	0.0028 (~1 every 355bp)	-	-	-	-
Total number of indels	18	-	-	-	-
Number of indels in CDS	6	-	-	-	-
Number of indels causing frameshift	4	-	-	-	-

# OF SPs	WHOLE mtDNA	CDS
Males	234 (160)	136 (107)
Males (no mRDI01)	84 (15)	32 (6)
Females	97 (23)	38 (9)

Table 8(on next page)

Indels located in coding sequences.

DEPTH = sequencing depth; QUAL = quality of the called SNP expressed in Phred score; ALLELE FREQUENCY = frequency of the alternative allele in each sample indicated in the "SAMPLE" column.

Table 8 Indels located in coding sequences. DEPTH = sequencing depth; QUAL = quality of the called SNP expressed in Phred score; ALLELE FREQUENCY = frequency of the alternative allele in each sample indicated in the "SAMPLE" column.

POSITION	DEPTH	QUAL	GENE	SNP	FRAMESHIFT	SAMPLE	ALLELE FREQUENCY	NOTES
1,698	3,732	1.38E+04	*cox1*	C/CAAA	No	mRDI02, mRDI03	0.089, 0.85	Insertion of 1 Lysine
6,364	1,929	2.15E+09	*cytb*	CT/C	Yes	fRDI04, mRDI05	0.80, 0.81	Yields a shorter Cytb. Possible sequencing error due to the homopolymer CTTTTTTT
10,449	1,780	2.15E+09	*nd5*	C/CT	Yes	fRDI01, fRDI04, fRDI05	0.11, 0.10, 0.11	Yields a nd5 gene divided in 2 ORFs. Possible sequencing error due to the homopolymer CTTTTTT
17,619	2,272	5.98E+03	*cox3*	AGCG/A	No	mRDI01	0.97	Deletion of 1 Alanine
17,621	2,188	9.99E+04	*cox3*	CG/C	Yes	mRDI01	0.99	Always combined with SNP_17624. Together change the last 35 amino acids.
17,624	2,287	5.98E+03	*cox3*	C/CAT	Yes	mRDI01	0.99	Always combined with SNP_17621. Together change the last 35 amino acids.